Vortex Trapping: a pathway to planet formation in low metallicities?

The Astrophysical Journal, 913:92 (14pp), 2021 June 1 https://doi.org/10.3847/1538-4357/abf739

Pebble Trapping in Vortices: Three-dimensional Simulations

Natalie Raettig[1], Wladimir Lyra[2], and Hubert Klahr[1]
[1] Max-Planck-Institut für Astronomie, Königstuhl 17, D-69117, Heidelberg, Germany
[2] New Mexico State University, Department of Astronomy, P.O. Box 30001 MSC 4500, Las Cruces, NM 88001, USA; wlyra@nmsu.edu
Received 2020 December 24; revised 2021 March 30; accepted 2021 April 10; published 2021 May 28

Abstract

Disk vortices have been heralded as promising routes for planet formation due to their ability to trap significant amounts of pebbles. While the gas motions and trapping properties of two-dimensional vortices have been studied in enough detail in the literature, pebble trapping in three dimensions has received less attention, due to the higher computational demand. Here we use the PENCIL CODE to study 3D vortices generated by convective overstability and the trapping of solids within them. The gas is unstratified whereas the pebbles settle to the midplane due to vertical gravity. We find that for pebbles of normalized friction times of St = 0.05 and St = 1, and dust-to-gas ratio $\varepsilon = 0.01$, the vortex column in the midplane is strongly perturbed. Yet when the initial dust-to-gas ratio is decreased the vortices remain stable and function as efficient pebble traps. Streaming instability is triggered even for the lowest dust-to-gas ratio ($\varepsilon_0 = 10^{-4}$) and smallest pebble sizes (St = 0.05) we assumed, showing a path for planetesimal formation in vortex cores from even extremely subsolar metallicity. To estimate if the reached overdensities can be held together solely by their own gravity we estimate the Roche density at different radii. Depending on disk model and radial location of the pebble clump we do reach concentrations higher than the Roche density. We infer that if self-gravity was included for the pebbles then gravitational collapse would likely occur.

Unified Astronomy Thesaurus concepts: Protoplanetary disks (1300); Planet formation (1241); Planetary system formation (1257); Solar system formation (1530); Solar nebulae (1508); Circumstellar dust (236); Circumstellar matter (241); Circumstellar disks (235)

The Astrophysical Journal Letters, 970:L19 (7pp), 2024 July 20 https://doi.org/10.3847/2041-8213/ad5af6

Rapid Protoplanet Formation in Vortices: Three-dimensional Local Simulations with Self-gravity

Wladimir Lyra[1], Chao-Chin Yang (楊朝欽)[2], Jacob B. Simon[3], Orkan M. Umurhan[4,5], and Andrew N. Youdin[6,7]
[1] New Mexico State University, Department of Astronomy, PO Box 30001 MSC 4500, Las Cruces, NM 88001, USA; wlyra@nmsu.edu
[2] Department of Physics and Astronomy, The University of Alabama, Box 870324, Tuscaloosa, AL 35487-0324, USA
[3] Department of Physics and Astronomy, Iowa State University, Ames, IA 50010, USA
[4] NASA Ames Research Center, Space Sciences Division, Planetary Sciences Branch, Moffatt Field, CA 94035, USA
[5] SETI, Carl Sagan Center, 190 Bernardo Way, Mountain View, CA 94043, USA
[6] Department of Astronomy and Steward Observatory, University of Arizona, Tucson, AZ 85721, USA
[7] The Lunar and Planetary Laboratory, University of Arizona, Tucson, AZ 85721, USA
Received 2024 February 22; revised 2024 June 11; accepted 2024 June 24; published 2024 July 19

Abstract

Disk vortices, seen in numerical simulations of protoplanetary disks and found observationally in Atacama Large Millimeter/submillimeter Array and Very Large Array images of these objects, are promising sites for planet formation given their pebble trapping abilities. Previous works have shown a strong concentration of pebbles in vortices, but gravitational collapse has only been shown in low-resolution, two-dimensional, global models. In this Letter, we aim to study the pebble concentration and gravitational collapse of pebble clouds in vortices via high-resolution, three-dimensional, local models. We performed simulations of the dynamics of gas and solids in a local shearing box where the gas is subject to convective overstability, generating a persistent giant vortex. We find that the vortex produces objects of Moon and Mars mass, with a mass function of power-law $d\ln N/d\ln M = -1.6 \pm 0.3$. The protoplanets grow rapidly, doubling in mass in about five orbits, following pebble accretion rates. The mass range and mass doubling rate are in broad agreement with previous low-resolution global models. We conclude that Mars-mass planetary embryos are the natural outcome of planet formation inside the disk vortices seen in millimeter and radio images of protoplanetary disks.

Unified Astronomy Thesaurus concepts: Planet formation (1241)

Pizza Lunch 09/30/24

Vortex Trapping: a pathway to planet formation in low metallicities?

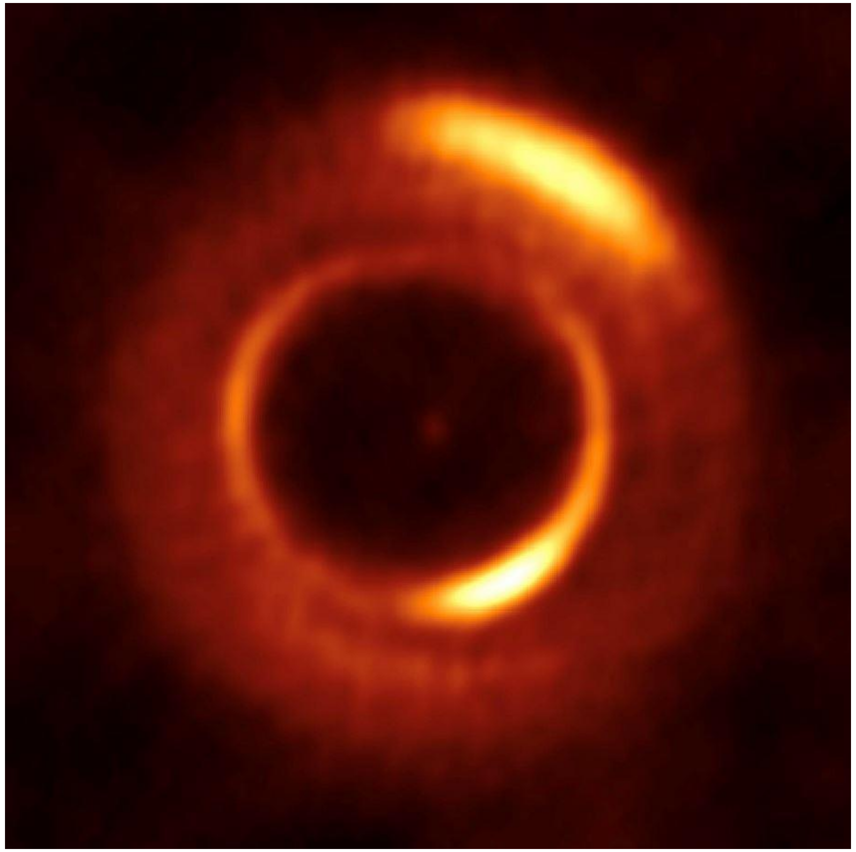

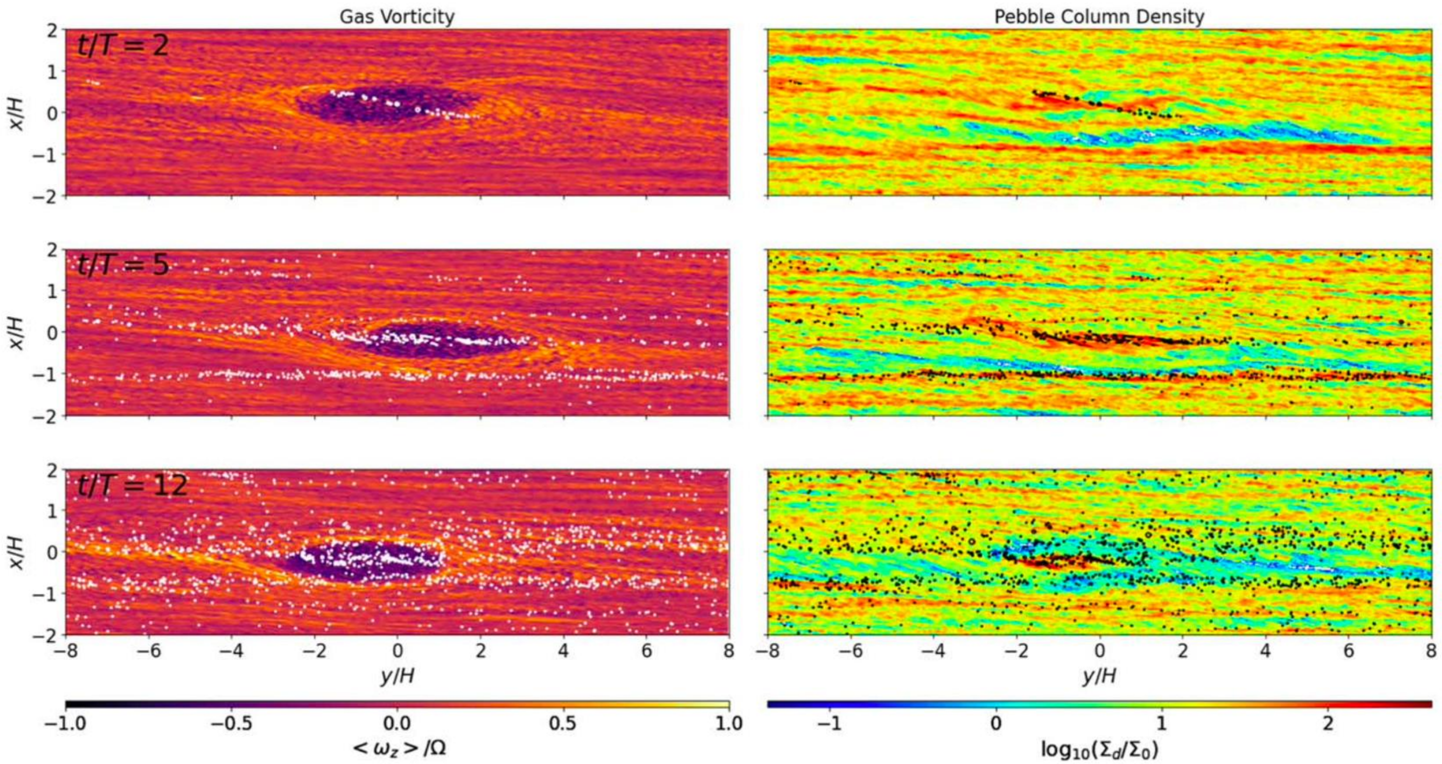

Headwind and Dust Drift

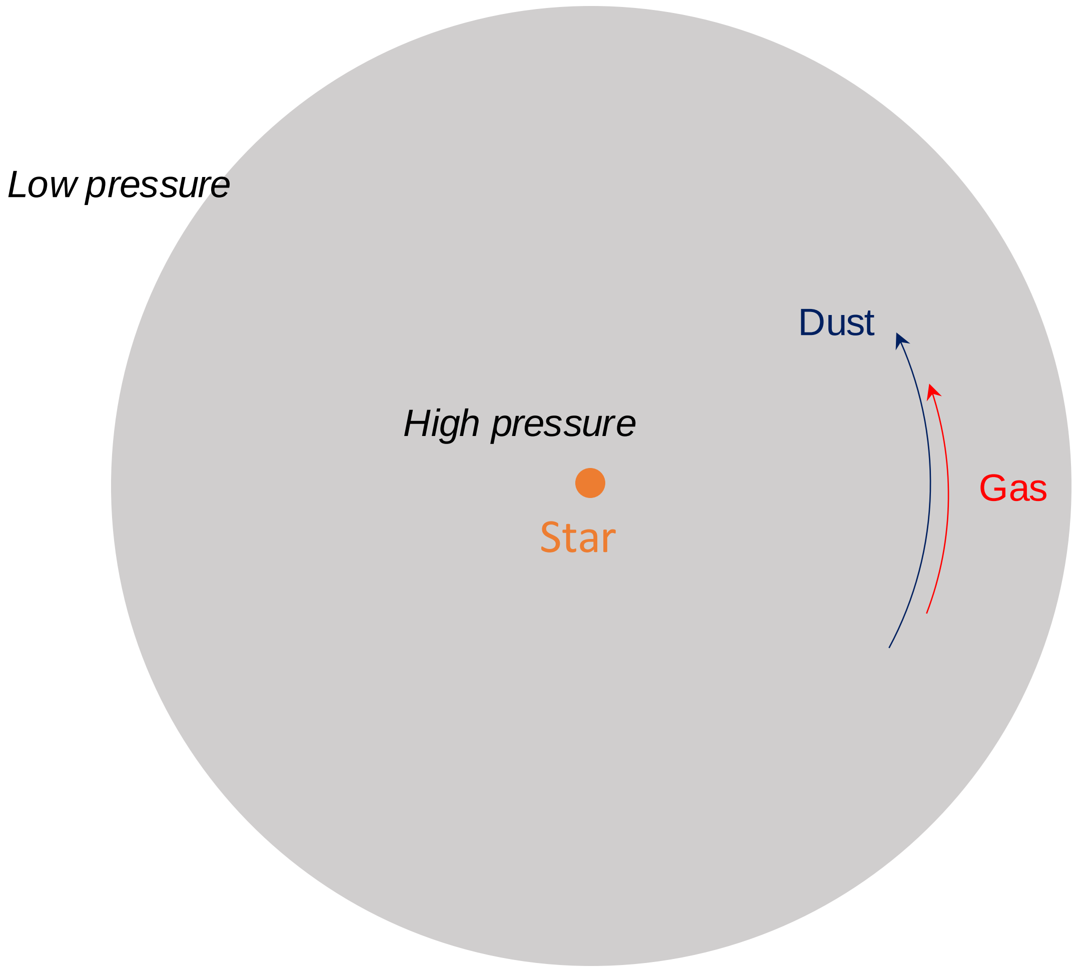

The gas has some pressure support (sub-Keplerian).

The dust does not feel gas pressure (Keplerian).

Streaming Instability

The dust drift is hydrodynamically unstable

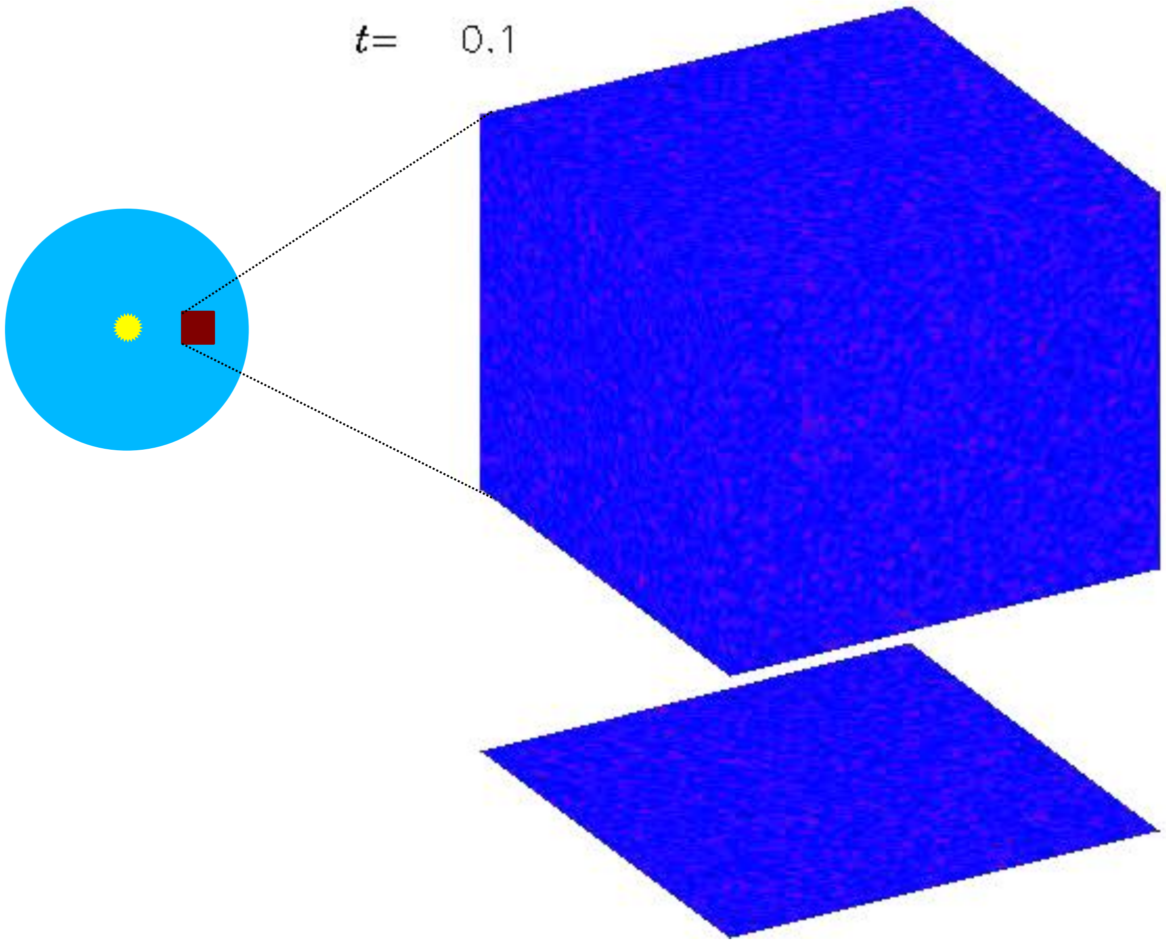

Youdin & Goodman '05, Johansen & Youdin '07, Youdin & Johansen+ '07, Kowalik+ '13, Lyra & Kuchner '13,
Schreiber+ '18, Klahr & Schreiber '20, Simon+ '16, '17, Carrera+ '15, '17, '20, Gole+ '20, Li+ '18, '19, Abod+ '19, Nesvorny+ '19

Gravitational collapse into planetesimals

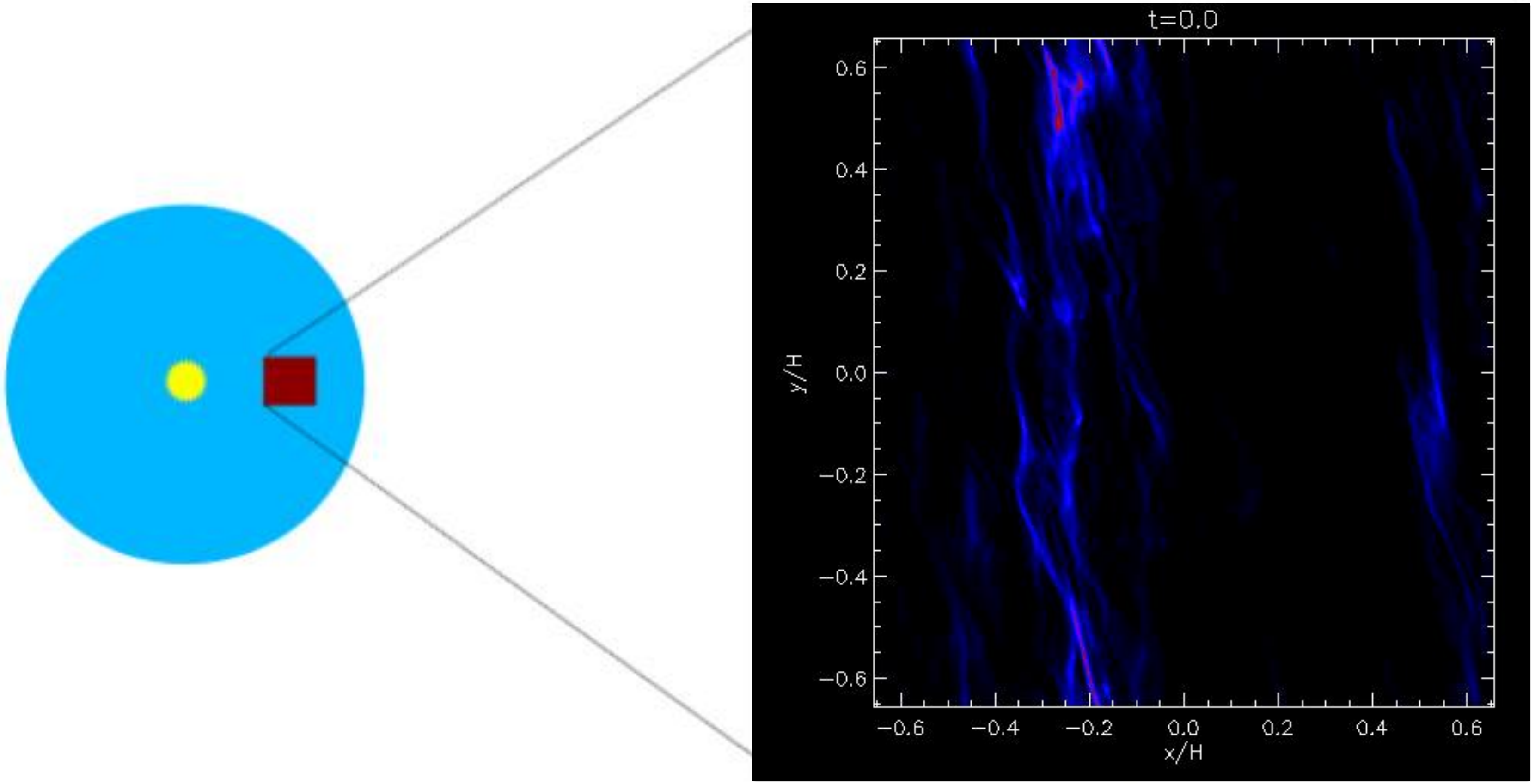

Johansen et al. (2007)

Metallicity threshold?

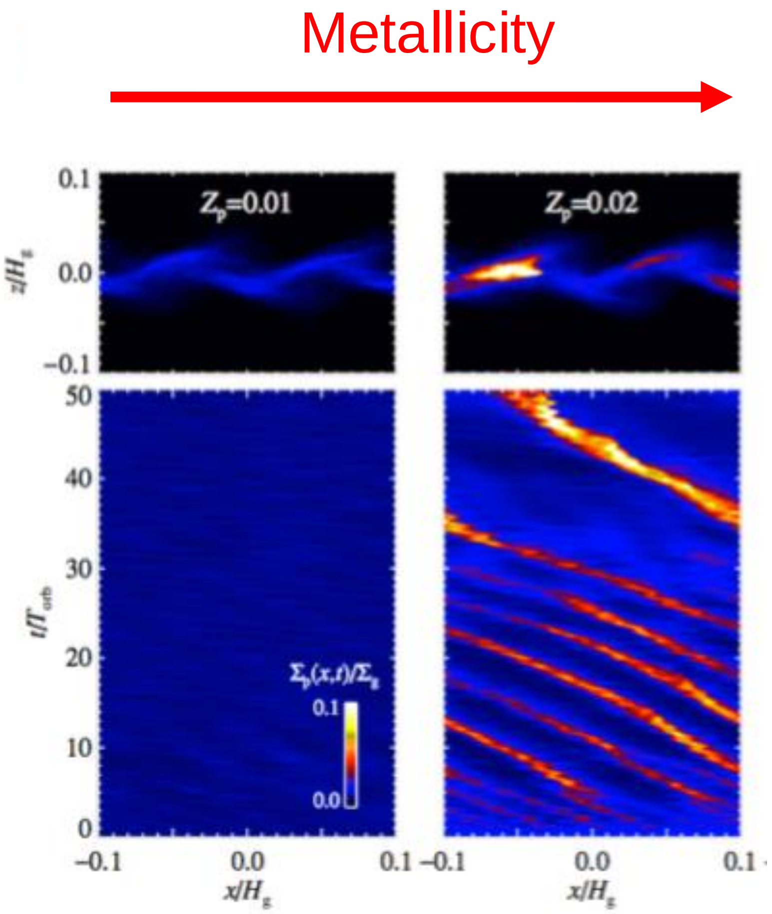

Johansen et al. (2011)

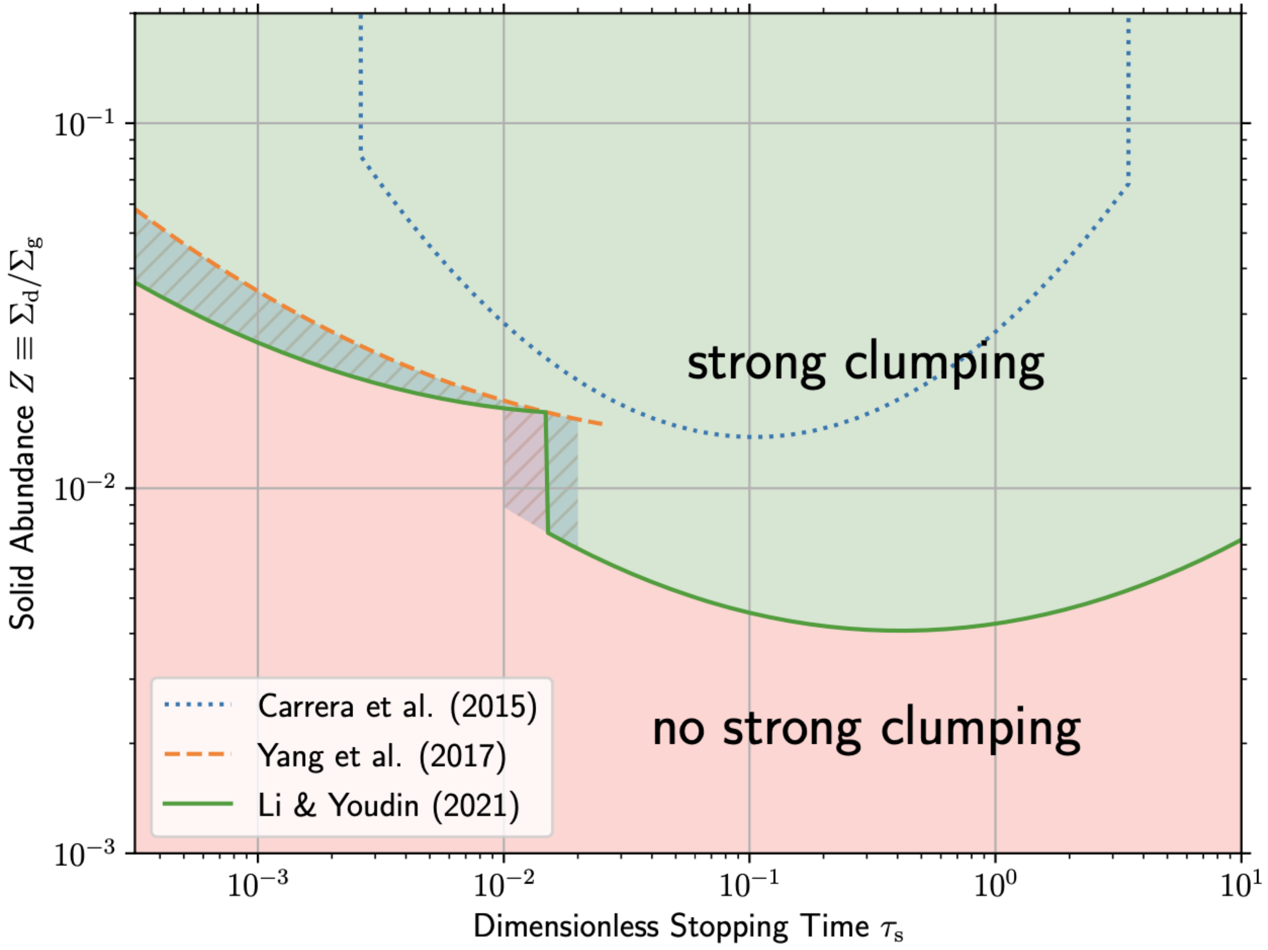

Lesur et al. 2023

Metallicity threshold?

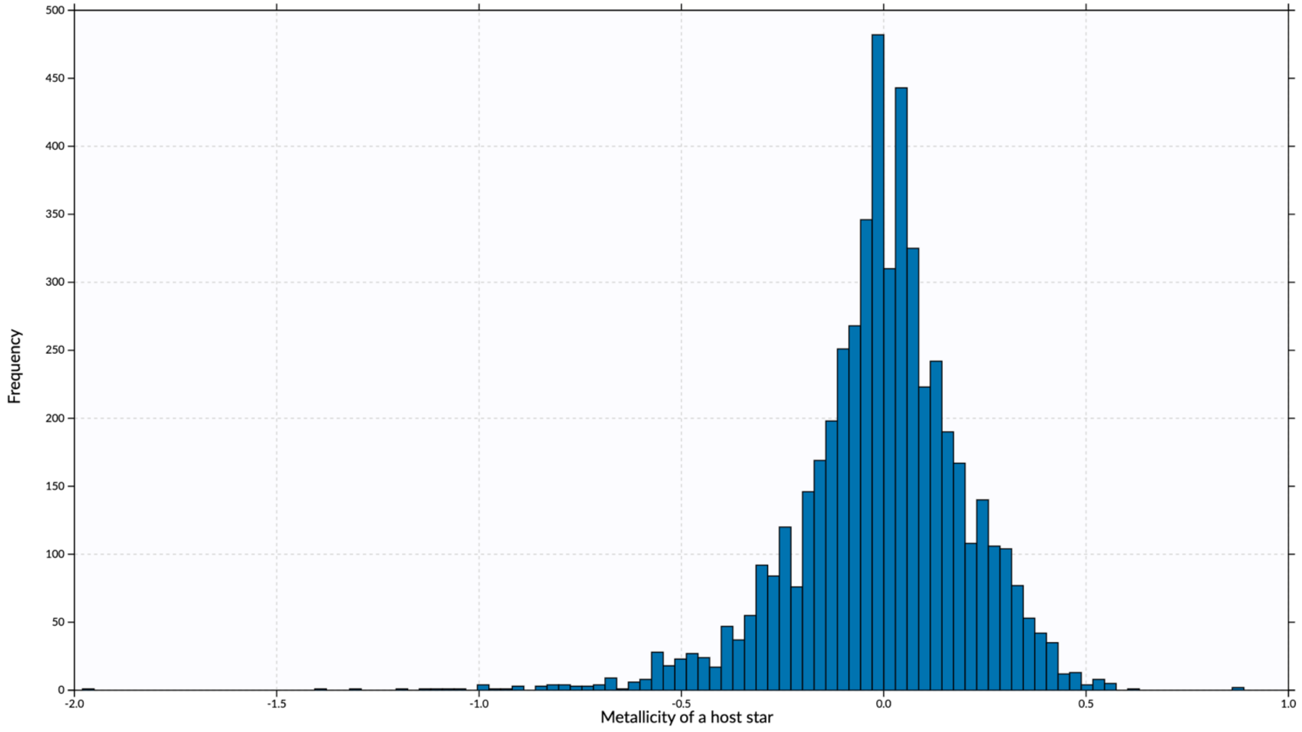

[Fe/H]

$Z = Z_{\odot}\, 10^{[Fe/H]}$

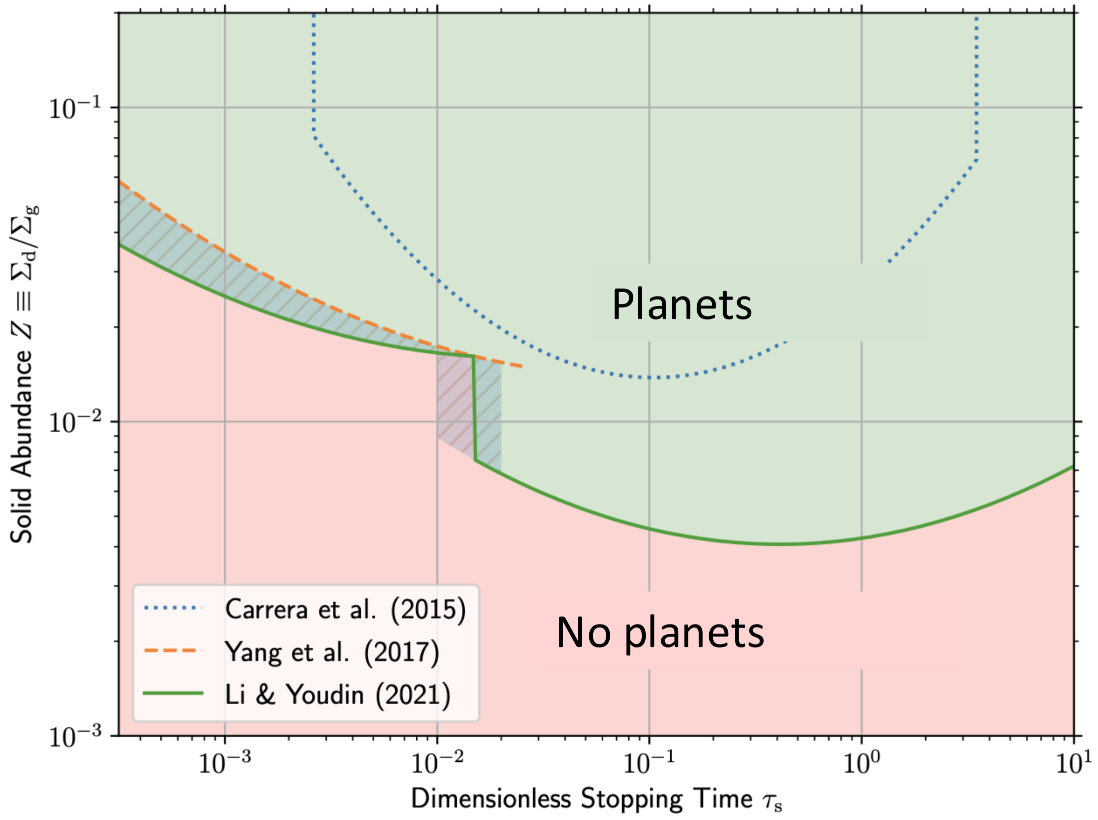

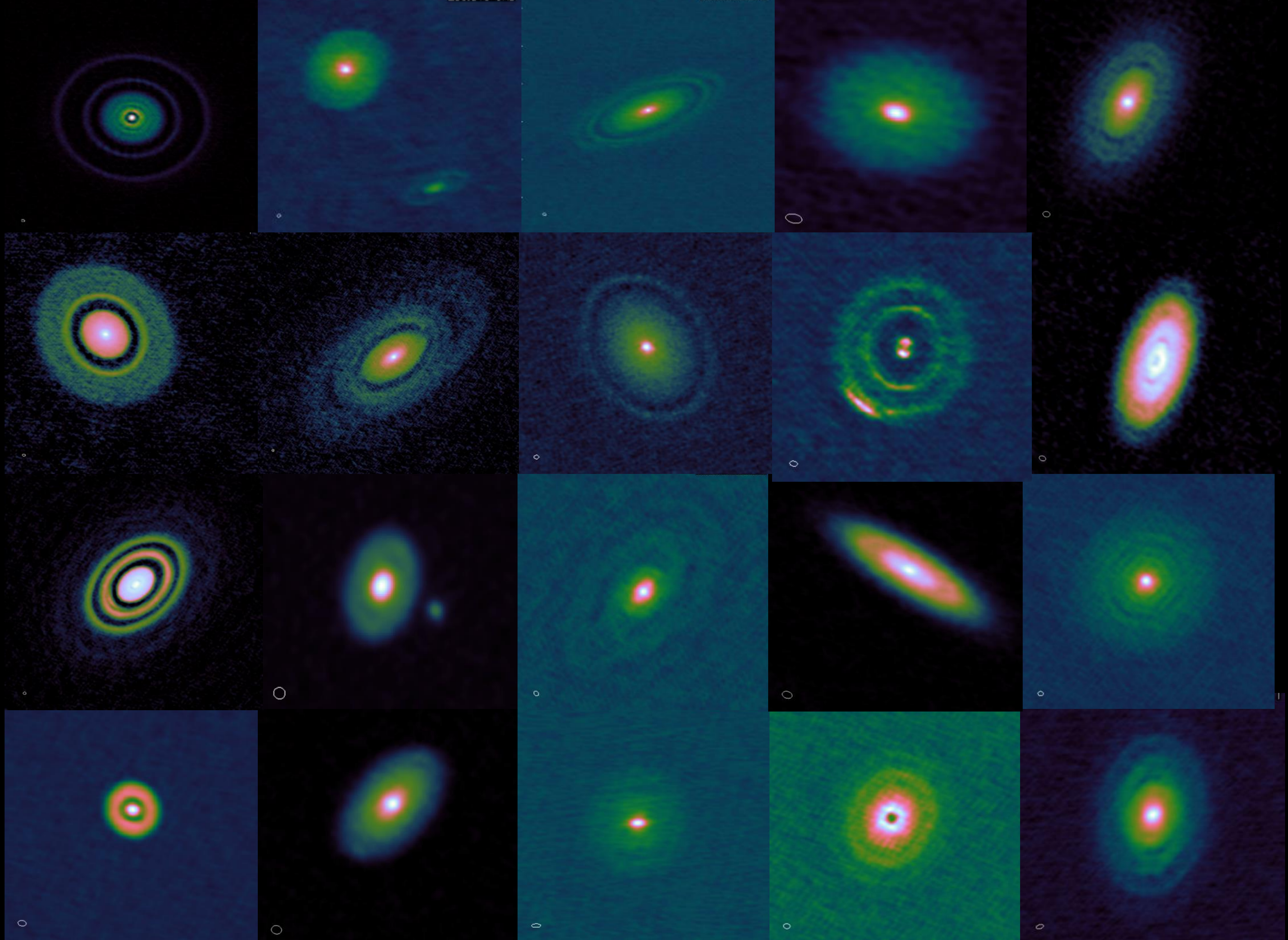

MWC 758

Vortex Trapping

Geostrophic balance:

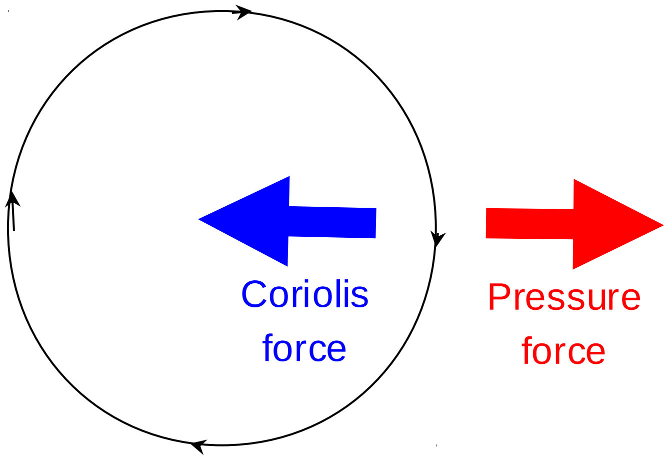

Vortex
streamline

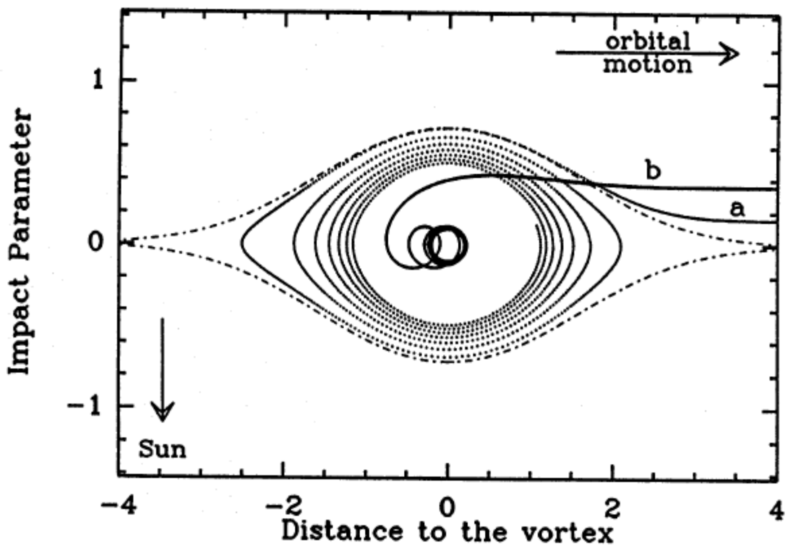

Barge & Sommeria (1995)

Grains do not feel the pressure gradient.
They sink towards the center, where they accumulate.

Aid to planet formation

(Barge & Sommeria 1995, Tanga et al. 1996, Barranco & Marcus 2005)

Speeds up planet formation enormously

(Lyra et al. 2008b, 2009ab, Raettig et al. 2012)

Vortex Formation: Convective Overstability

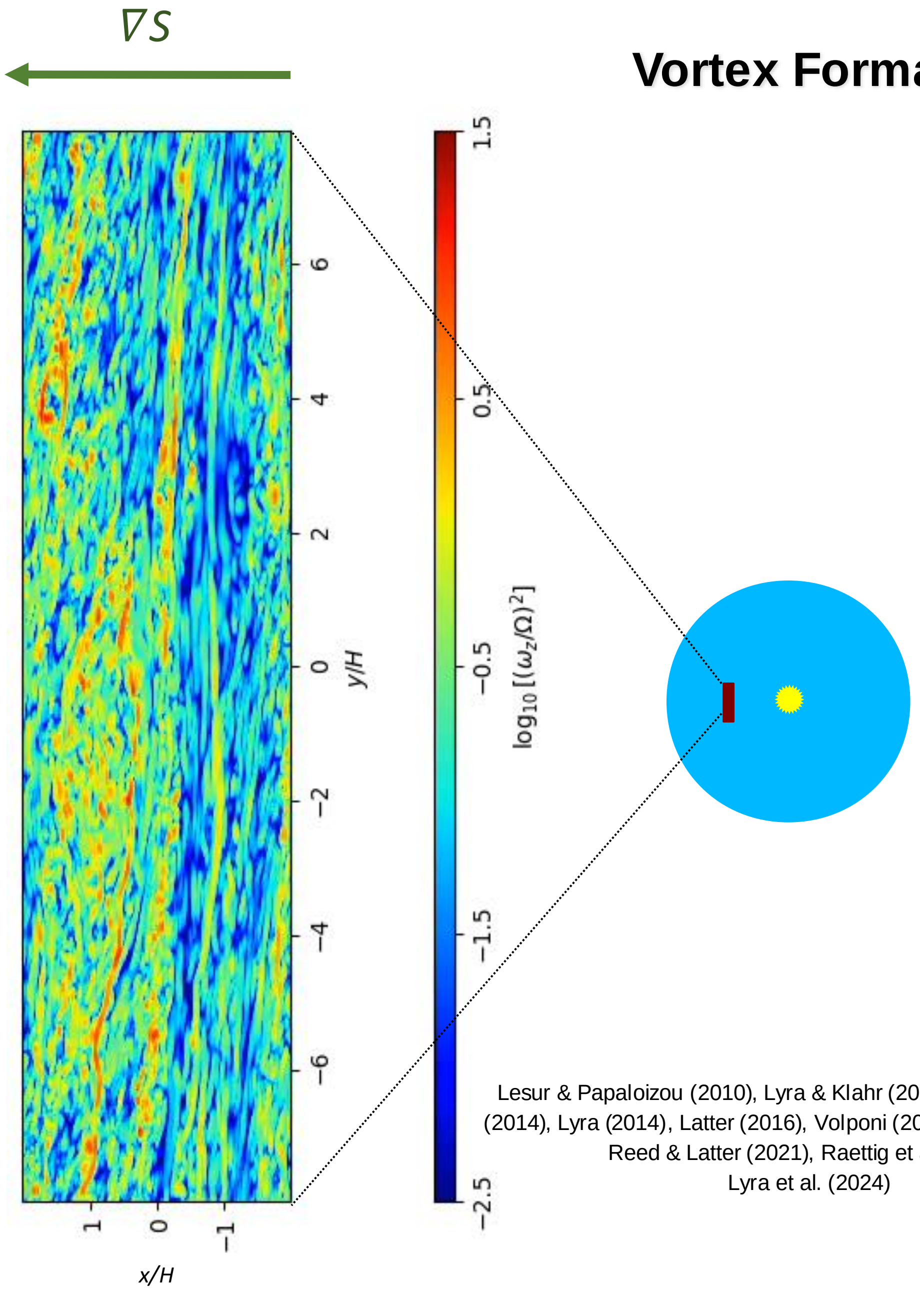

Lesur & Papaloizou (2010), Lyra & Klahr (2011), Klahr & Hubbard (2014), Lyra (2014), Latter (2016), Volponi (2016), Lyra et al. (2018), Reed & Latter (2021), Raettig et al. (2021)
Lyra et al. (2024)

Sketch of the
Convective Overstability

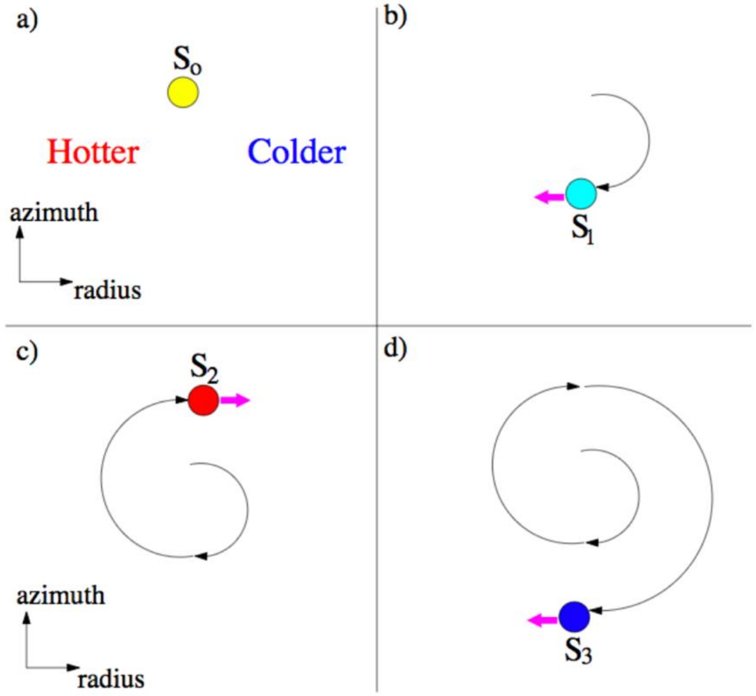

Latter (2016)

Pebble trapping in 3D vortices

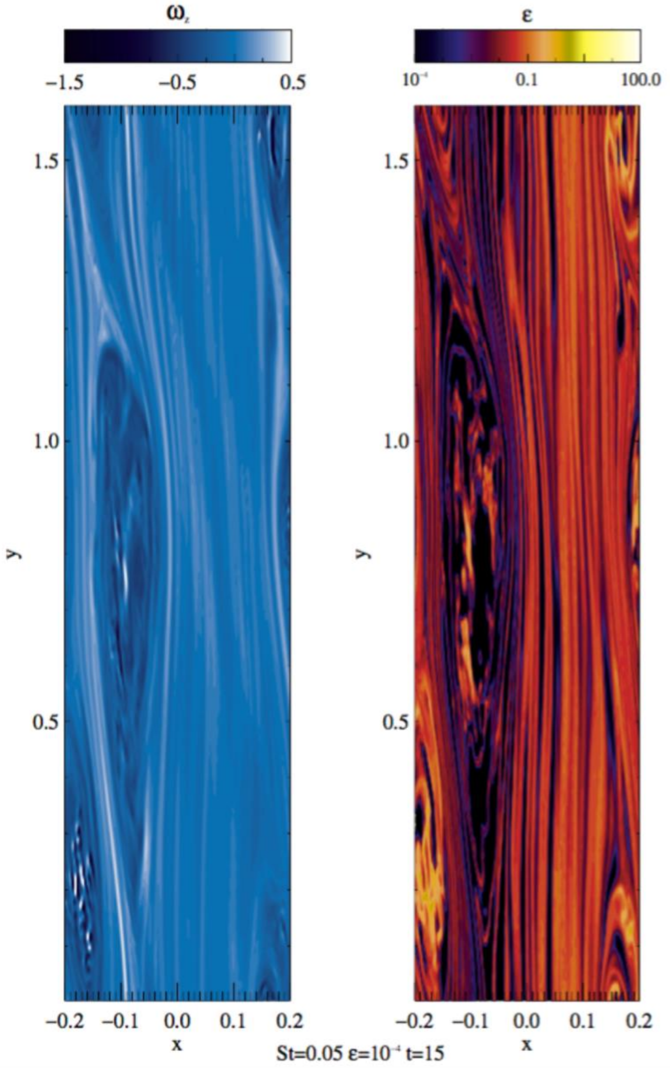

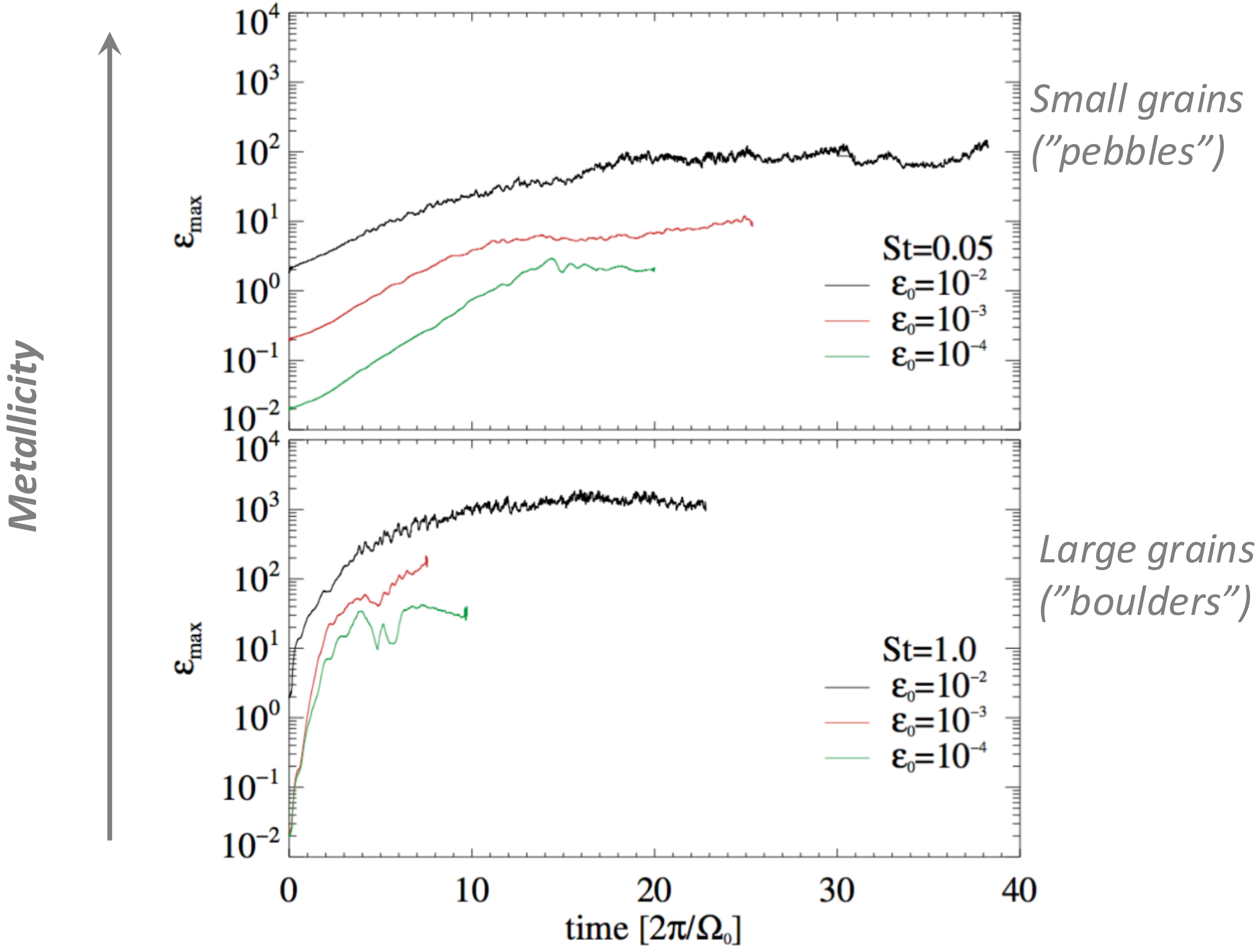

Raettig et al. (2021)

Gravitational Collapse

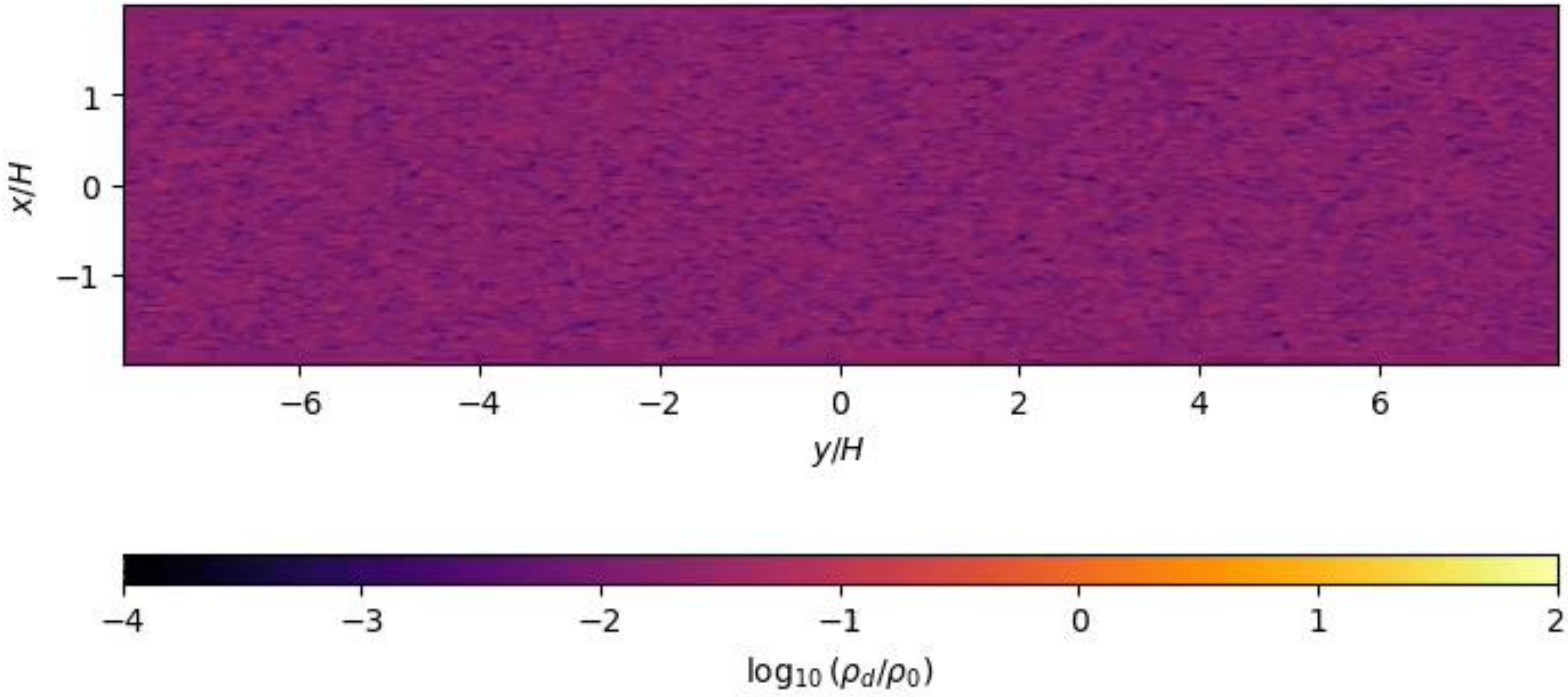

Lyra et al. (2024)

Timestep= 1 Time= 2513.300230

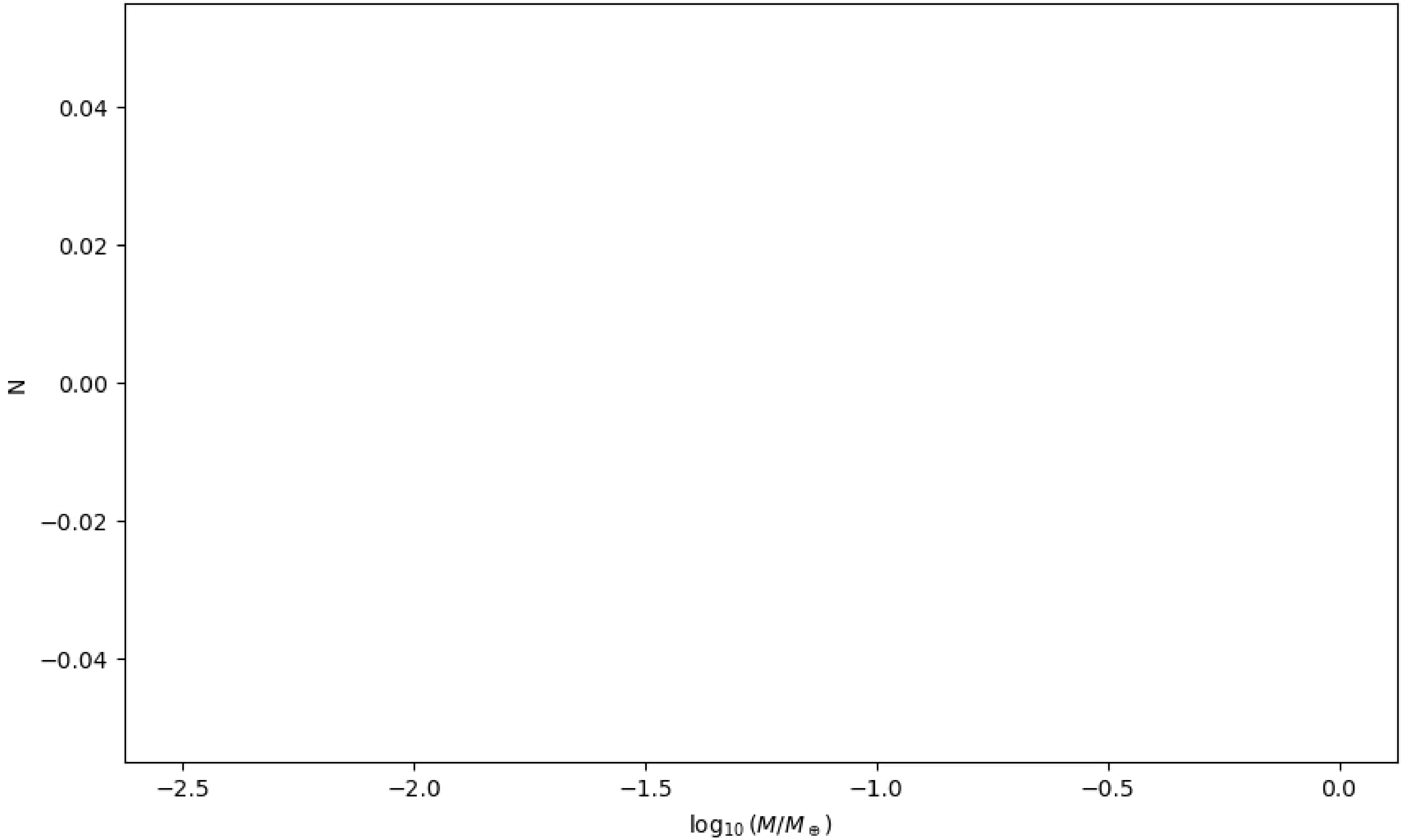

Gravitational Collapse - 512^3

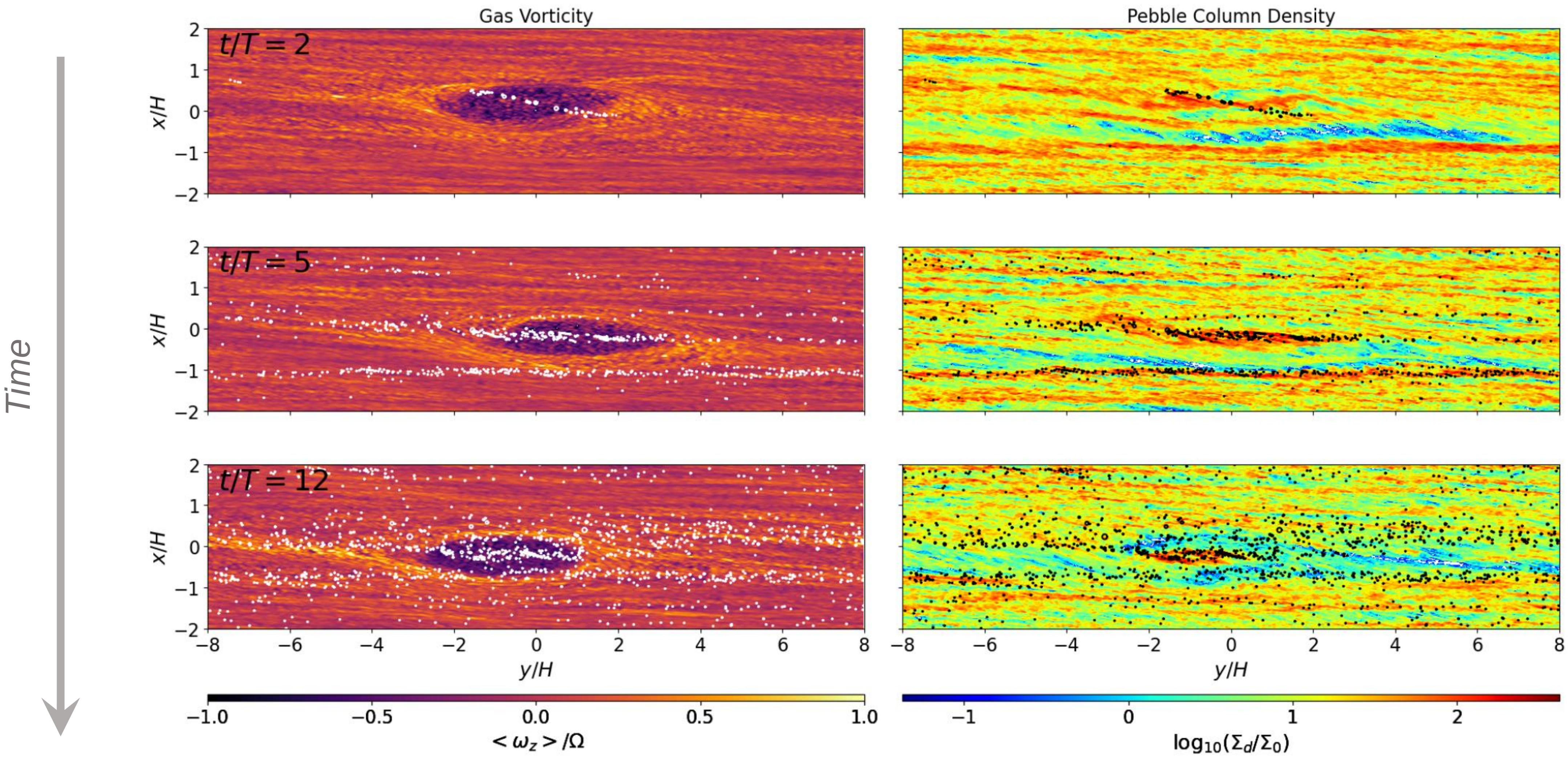

Lyra et al. (2024)

Gravitational Collapse – 256^3

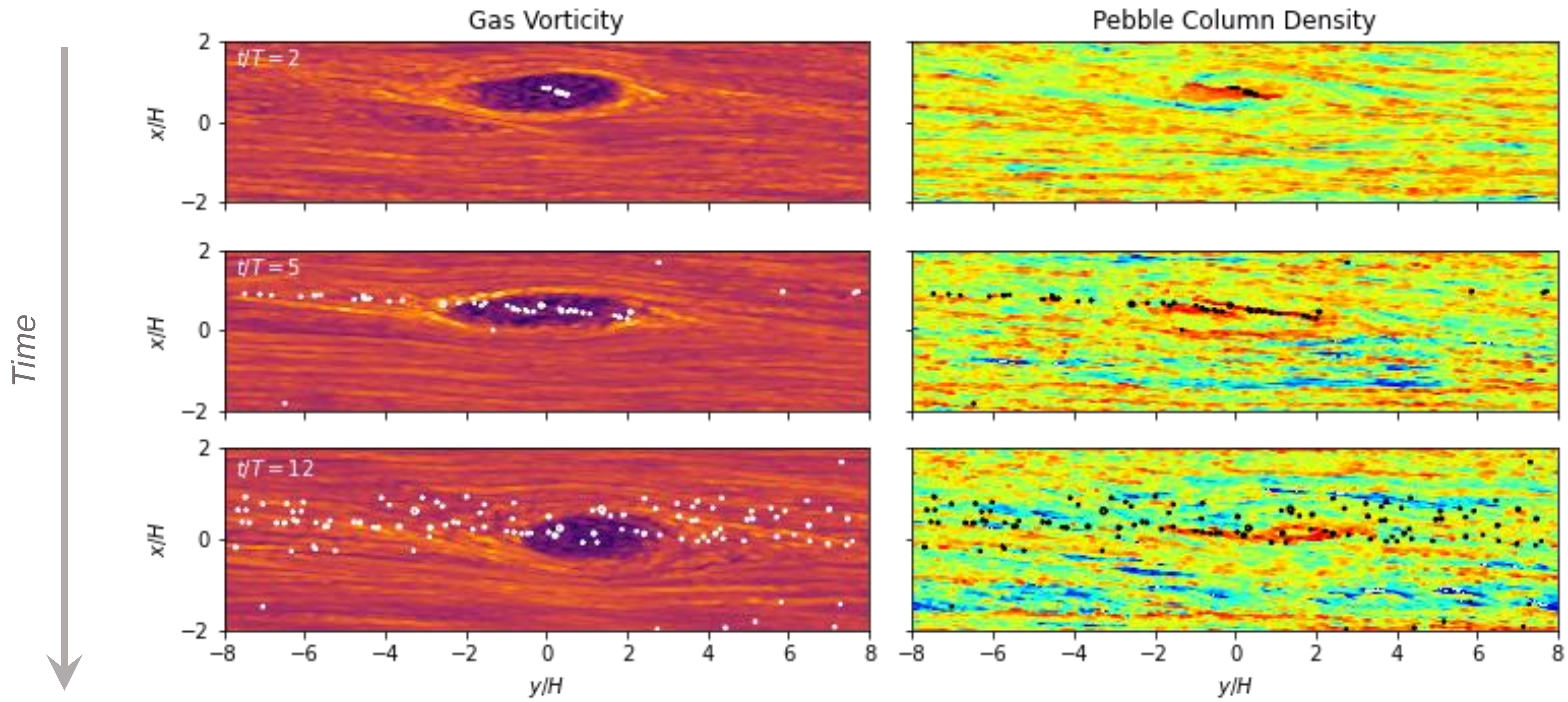

Lyra et al. (2024)

Convergence (or lack thereof)

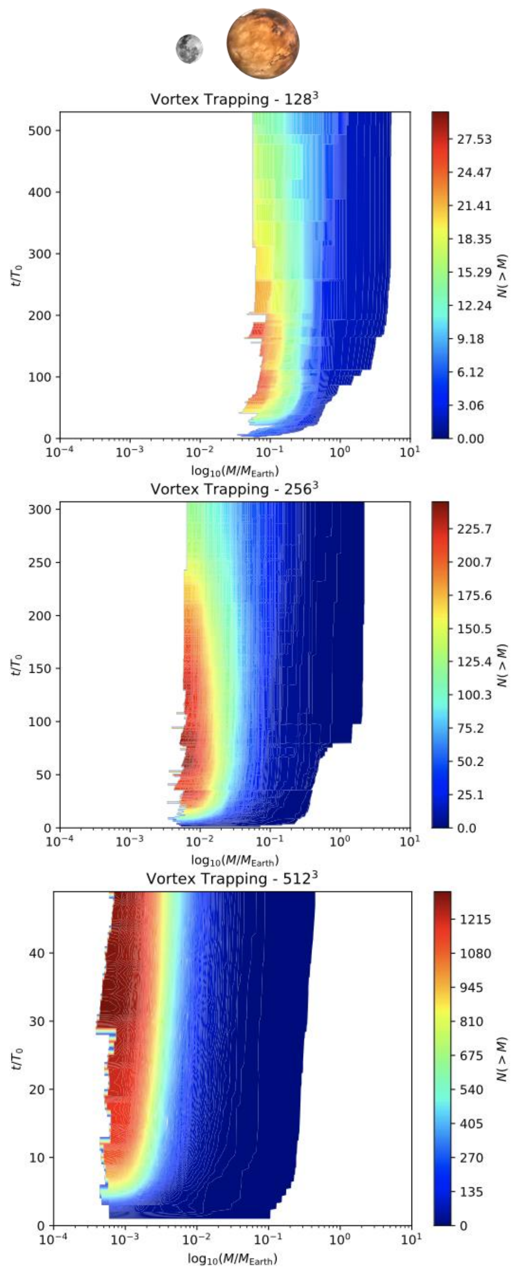

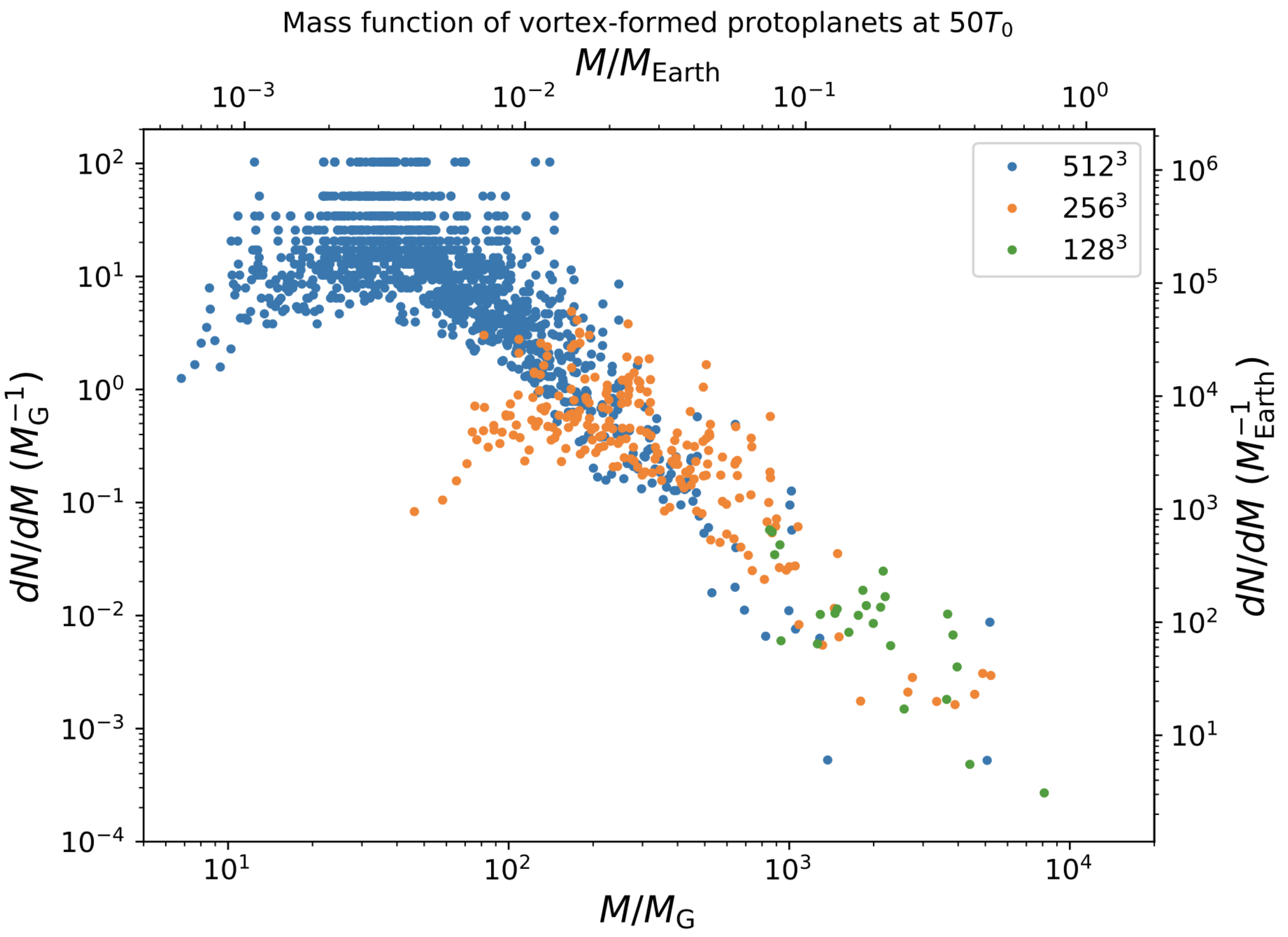

Lyra et al. (2024)

Convergence

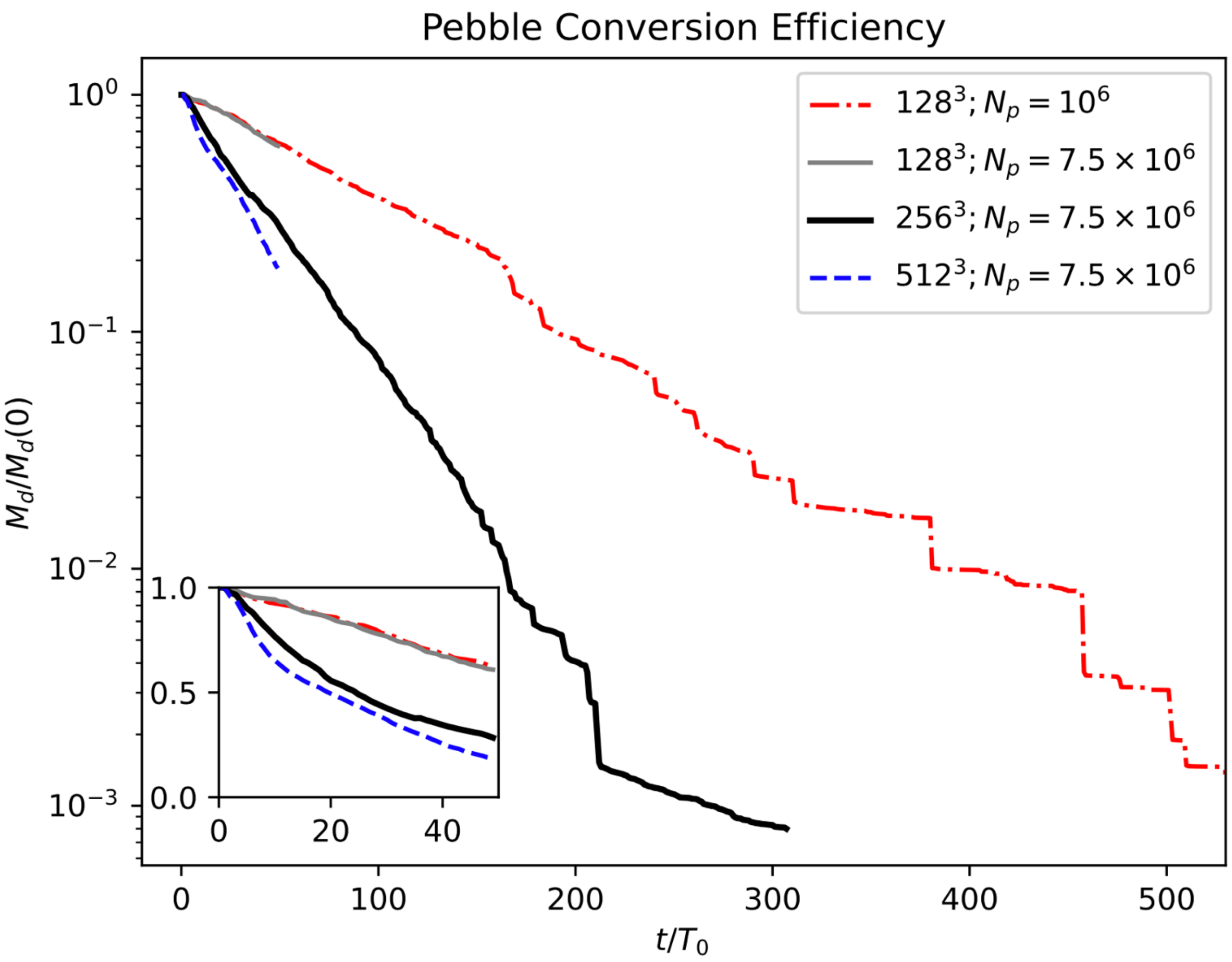

Lyra et al. (2024)

Limit to dust loading

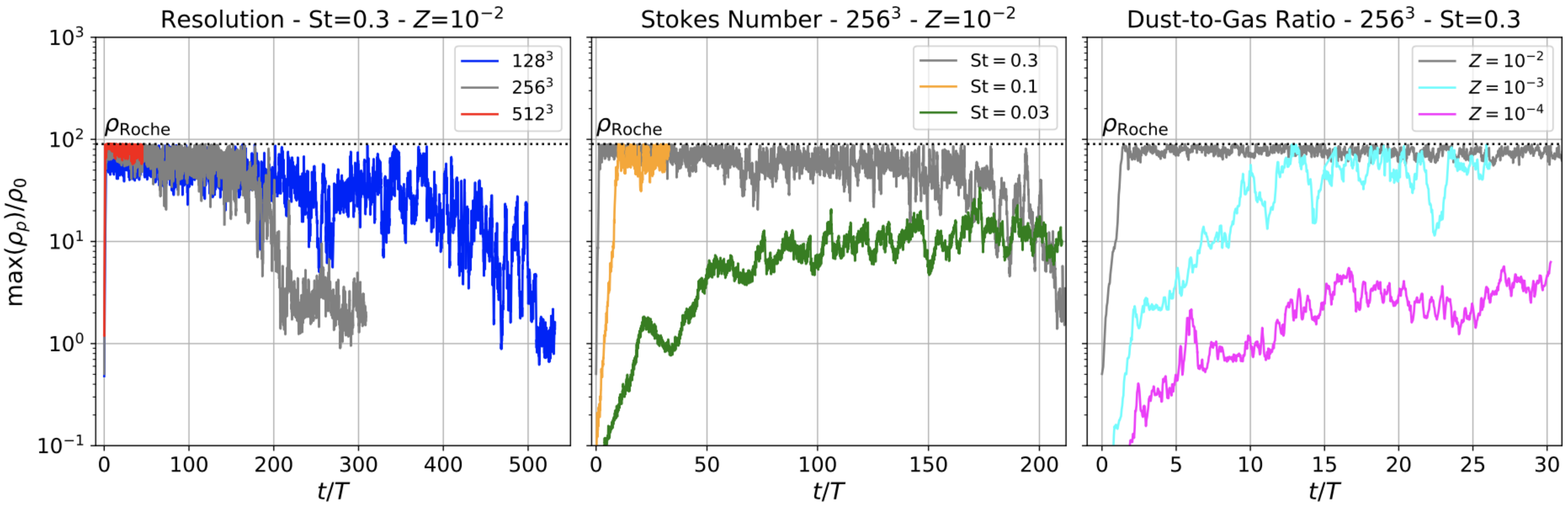

Lyra et al. (2024)

Drag-Diffusion Equilibrium

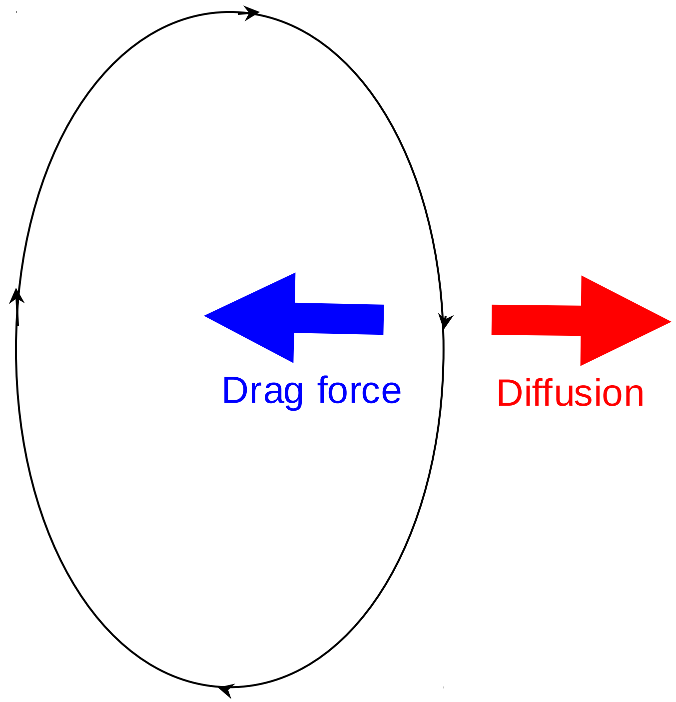

Trapped pebble

Dust continuity equation

$$\frac{\partial \rho_d}{\partial t} = -(\boldsymbol{v} \cdot \boldsymbol{\nabla})\rho_d - \rho_d \boldsymbol{\nabla} \cdot \boldsymbol{v} + D\nabla^2 \rho_d,$$

advection

compression

diffusion

Lyra & Lin (2013)

Analytical Solution for dust in Drag-Diffusion Equilibrium

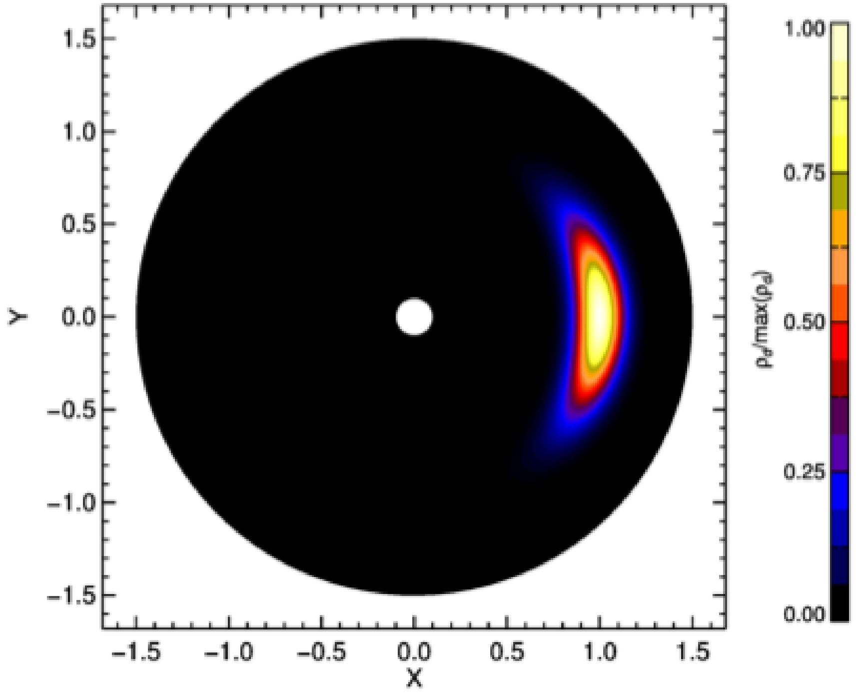

Solution for

H/r=0.1 χ*=4* *S*=1

Steady-state solution

$$\rho_d(a,z) = \varepsilon\rho_0 (S+1)^{3/2} \exp\left\{-\frac{[a^2 f^2(\chi)+z^2]}{2H^2}(S+1)\right\}$$

Lyra & Lin (2013)

$$S = \frac{St}{d}$$

$$\delta = v_{\rm rms}^2 / c_s^2,$$

a = vortex semi-minor axis
H = disk scale height (temperature)
χ = vortex aspect ratio
δ = diffusion parameter
St = Stokes number (particle size)
f(χ*)* = model-dependent scale function

Lyra & Lin (2013)

Vortices are quieter than the environment

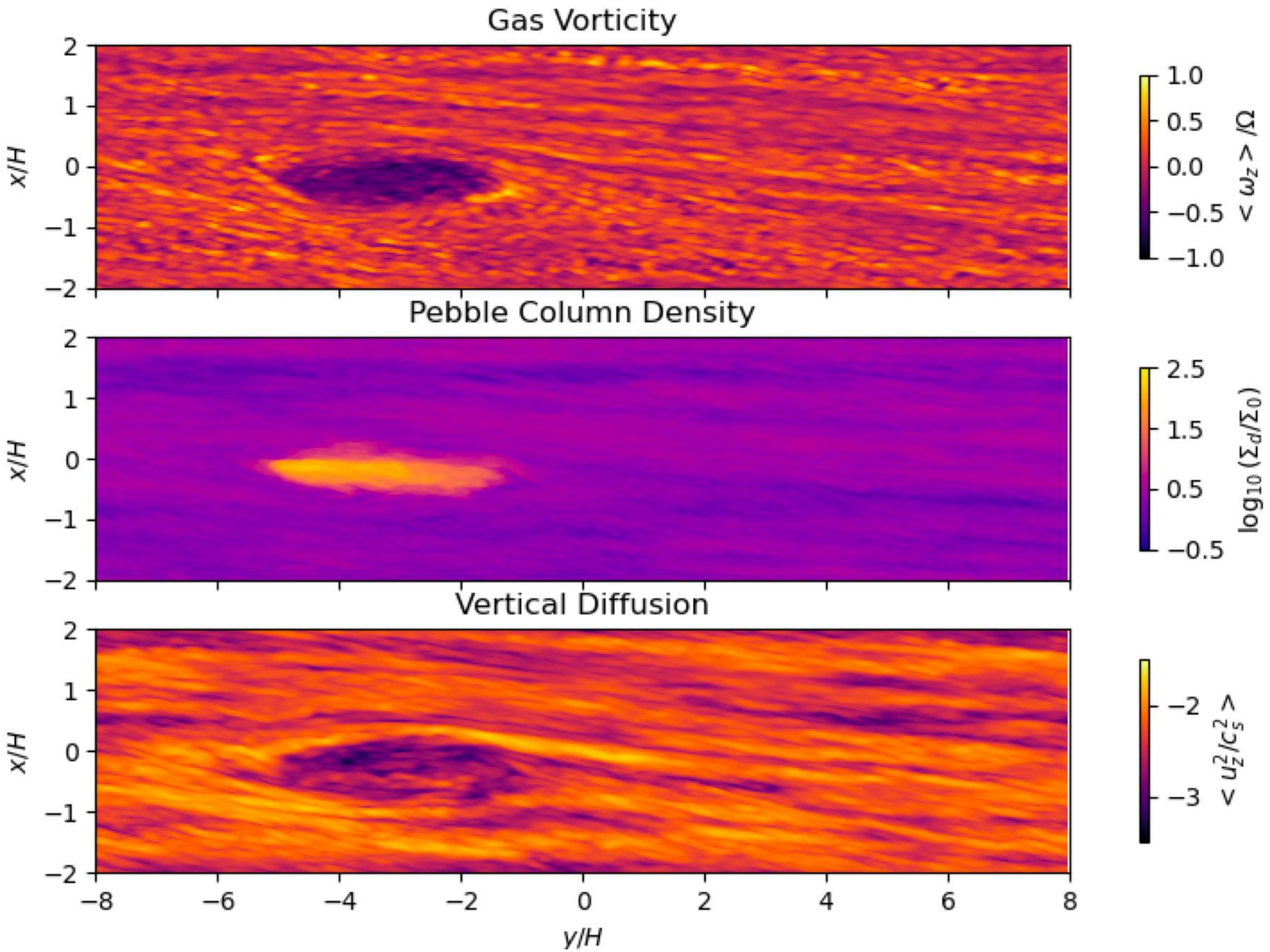

Dust loading dampens the turbulence

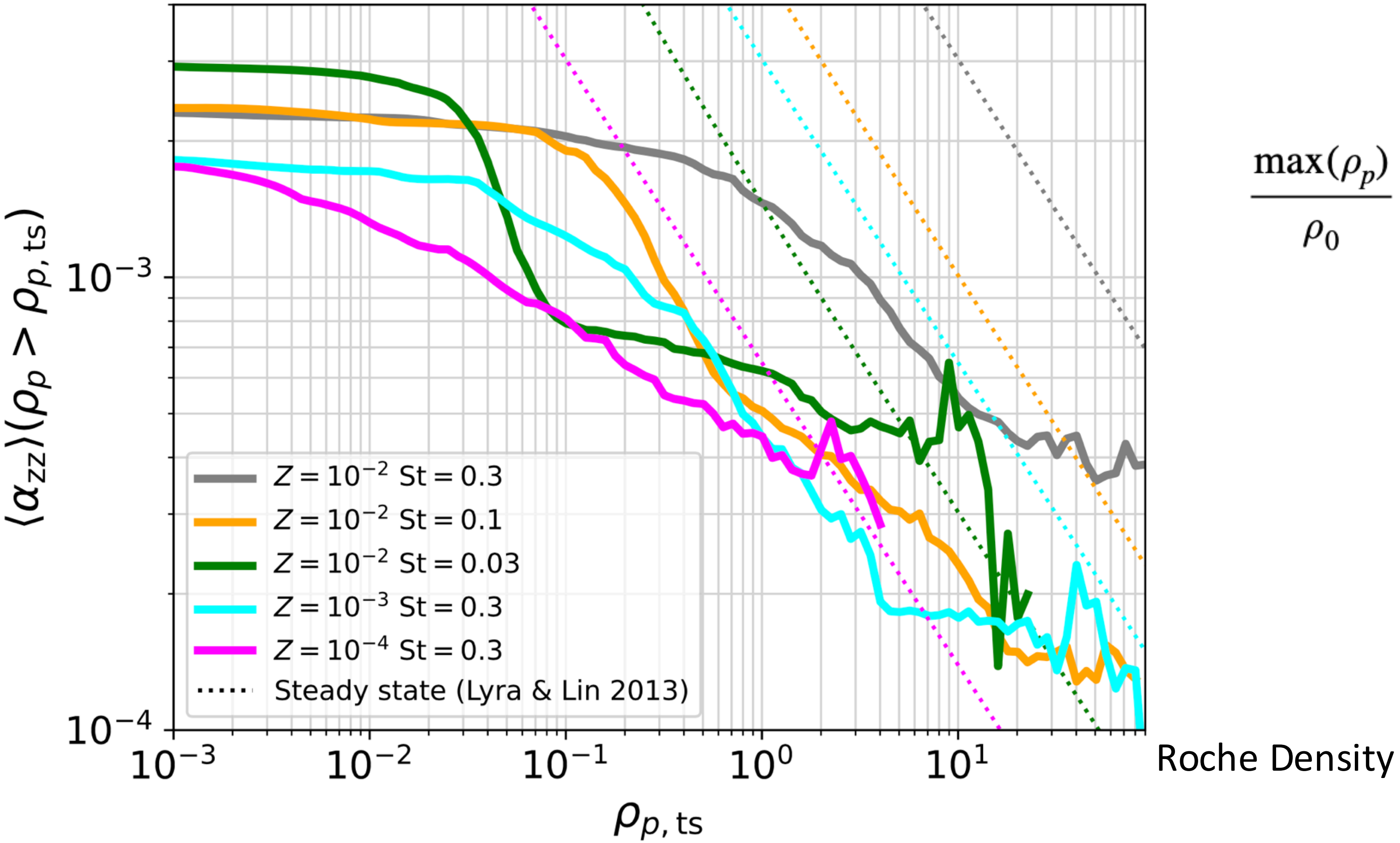

$$\frac{\max(\rho_p)}{\rho_0} = Z\left(\frac{\mathrm{St}}{\delta} + 1\right)^{1.5}$$

Lyra et al. (2024)

Vortex "Boost" – $Z = Z_0 (^{St}/_{\delta} + 1)$

Easily reaches dust-to-gas ratio > 1
even for solar (and sub-solar) metallicities.

$$\frac{\max(\rho_p)}{\rho_0} = Z\left(\frac{\mathrm{St}}{\delta} + 1\right)^{1.5}$$

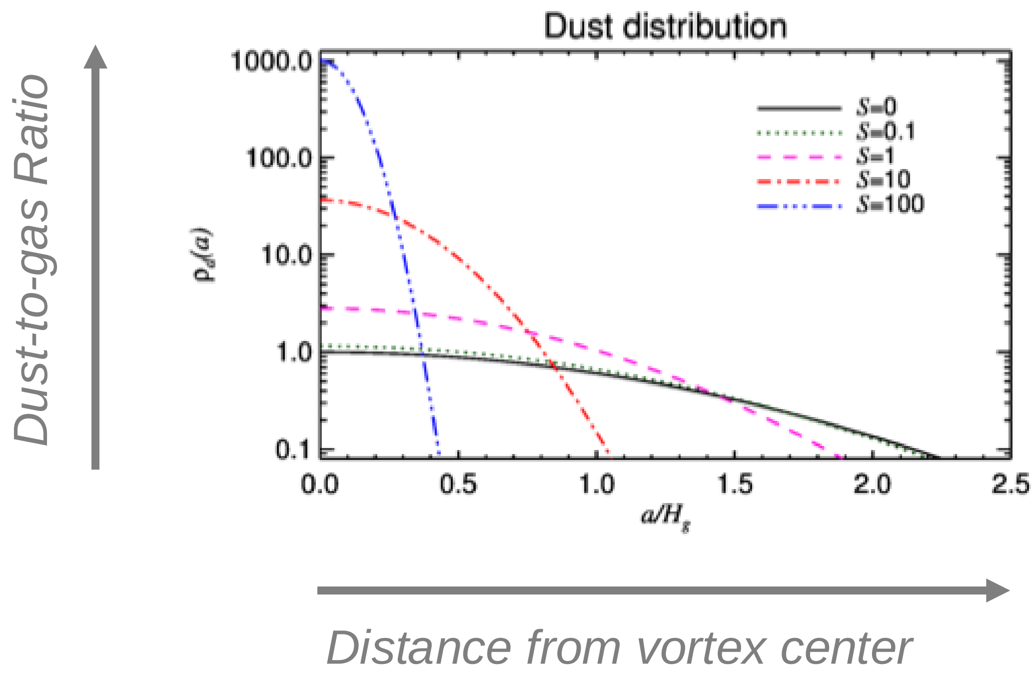

Lyra & Lin (2013)

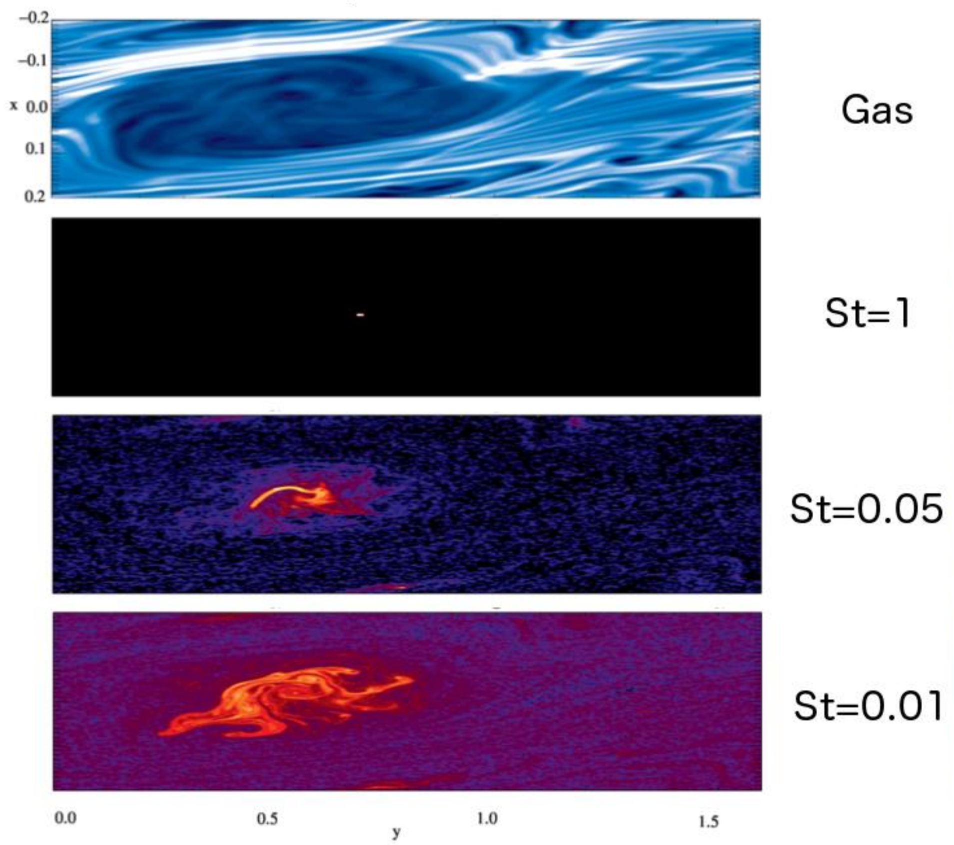

Raettig et al (2015)

Population II and Population III stars

Z (pop II): $10^{-4}\ Z_\odot \leq Z < 10^{-1}\ Z_\odot$
Z (pop III) ≈< $10^{-4}\ Z_\odot$

New simulations form solar-mass stars at zero metallicity

When did the first planet form?
When did the Universe start getting populated with planets?

$Z = Z_\odot\ 10^{[Fe/H]}$

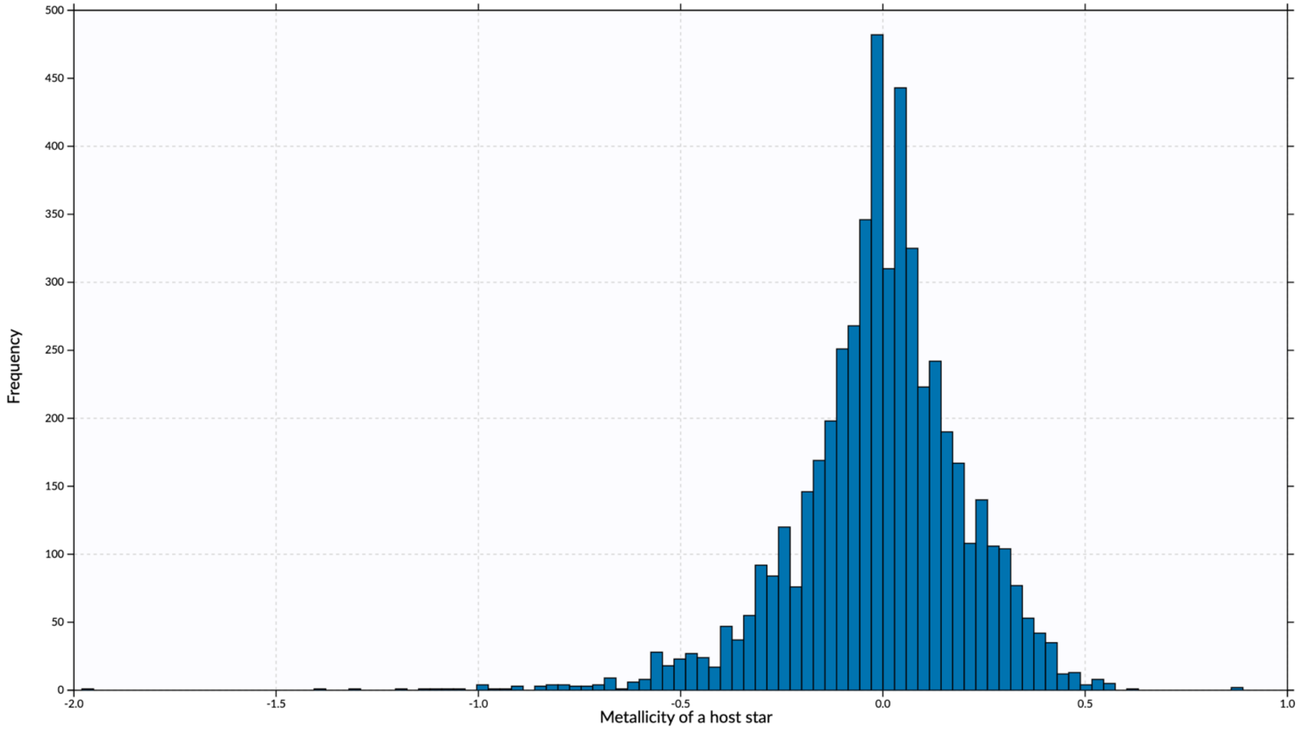

[Fe/H]

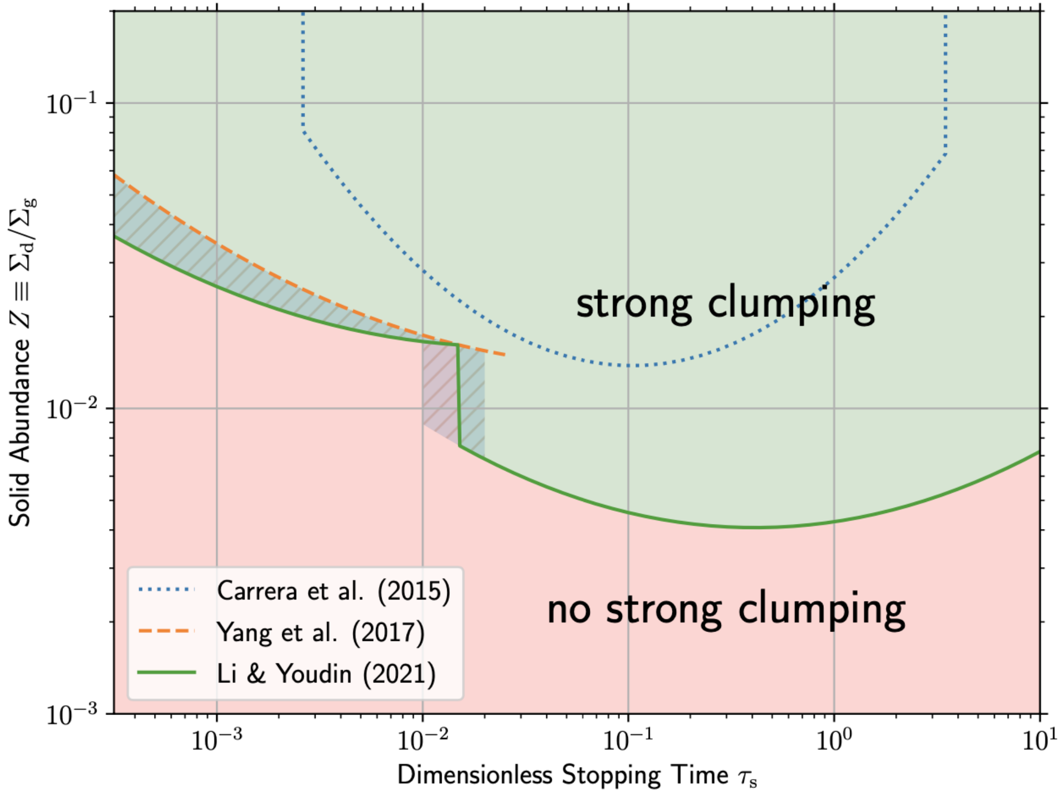

Metallicity – Redshift relationship

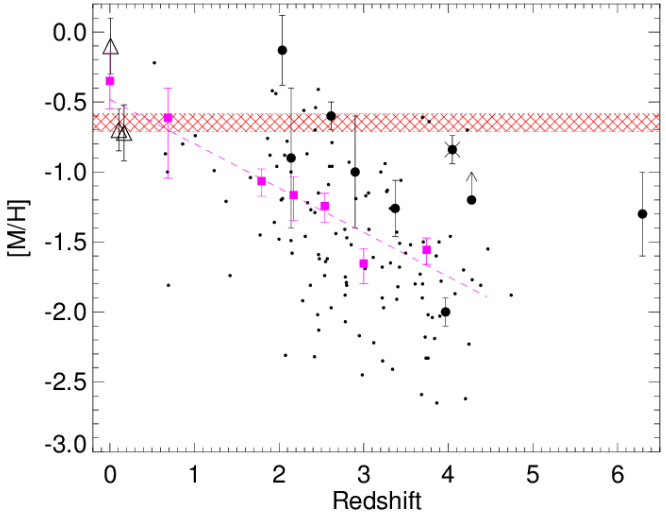

Metallicity as a function of redshift for different classes of objects. The black circles are the measurements for GRBs from Table 2 (GRB 060206 is also marked with ×). The open triangles show the metallicity of three low-z GRB host galaxies (Sollerman et al. 2005). The squares and the dashed line represent the column density weighted metallicity evolution derived by Zwaan et al. (2005, their Fig. 22). The small dots with no error-bars are measurements for 121 DLAs from Prochaska et al. (2003). The hatched region indicates the metallicity above which GRBs cannot form in the collapsar models.

Fynbo et al. (2006)

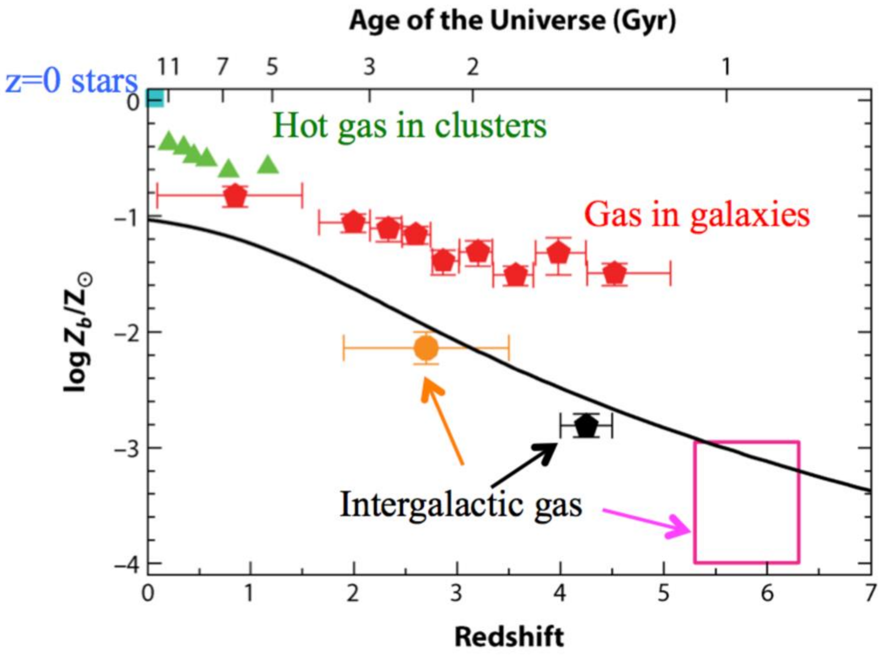

Figure 14: Mean metallicity of the Universe (in solar units): (*solid curve*) mass of heavy elements ever produced per cosmic baryon from our model SFH, for an assumed IMF-averaged yield of $y = 0.02$; (*turquoise square*) mass-weighted stellar metallicity in the nearby Universe from the SDSS (Gallazzi et al. 2008); (*green triangles*) mean iron abundances in the central regions of galaxy clusters (Balestra et al. 2007); (*red pentagons*) column density-weighted metallicities of the damped Lyα absorption systems (Rafelski et al. 2012); (*orange dot*) metallicity of the IGM as probed by O VI absorption in the Lyα forest (Aguirre et al. 2008); (*black pentagon*) metallicity of the IGM as probed by C IV absorption (Simcoe 2011); (*magenta rectangle*) metallicity of the IGM as probed by C IV and C II absorption (Ryan-Weber et al. 2009, Simcoe et al. 2011, Becker et al. 2011).

Madau & Dickinson (2014)

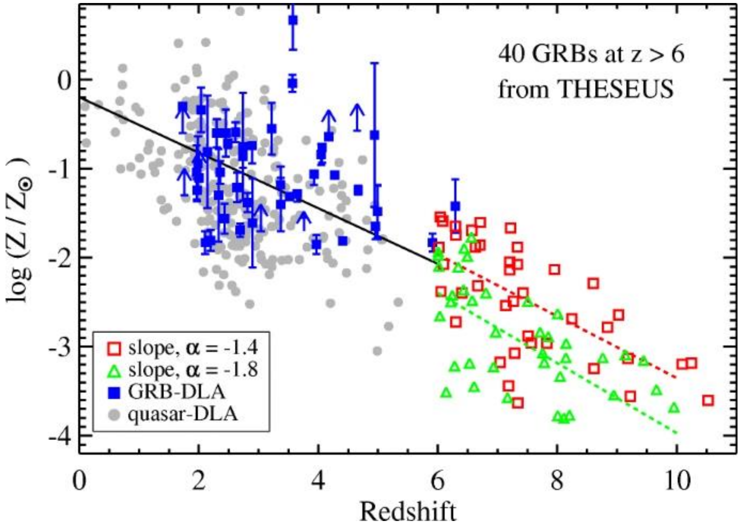

Absorption-line based metallicities relative to solar, corrected for dust depletion as a function of redshift for Quasar Damped Ly α absorbers (DLAs, grey symbols) and GRB-DLAs (blue symbols) (adapted from [97], [98]). Open square symbols show representative expectations for THESEUS, assuming continued evolution of the mass-metallicity relationship, and a dominant population of low mass galaxies at $z > 6$ (green triangles and red squares assume faint-end slopes of − 1.8 and − 1.4 for the galaxy luminosity function, respectively). GRBs represent the unique way for probing evolution of ISM absorption-based metallicities in the first billion years of cosmic history

Tanvir et al. (2021)

Low Metallicity

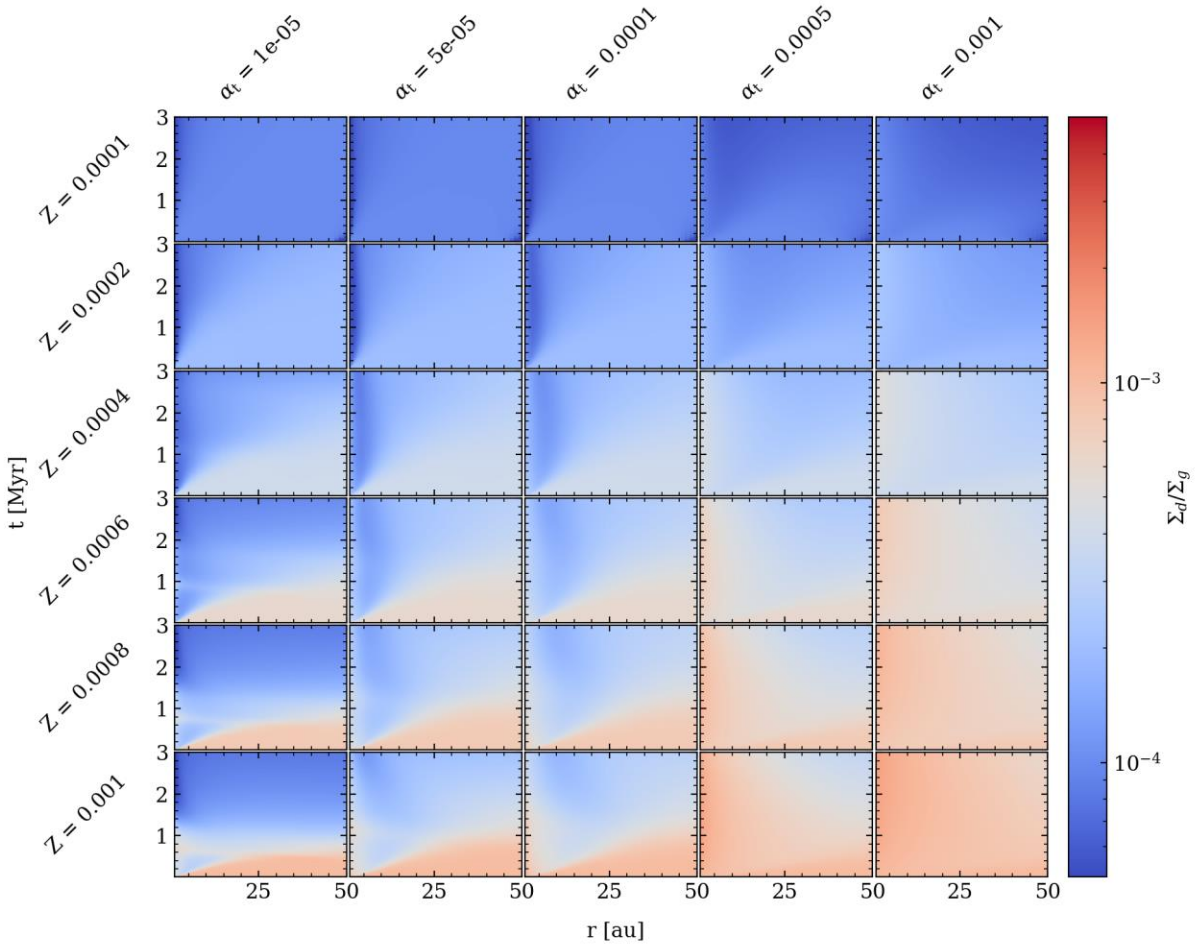

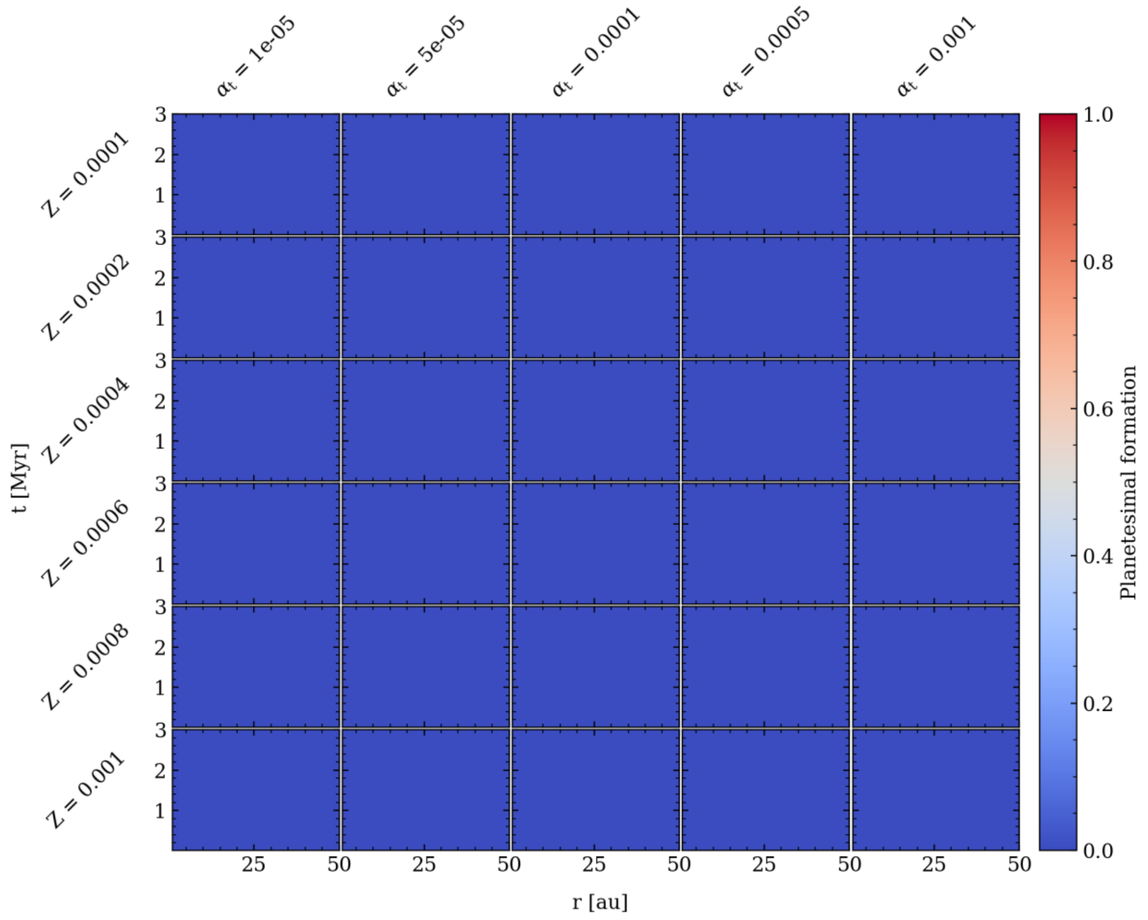

Vortex Boost

$$Z = Z_0\,({}^{St}/_{\delta} + 1)$$

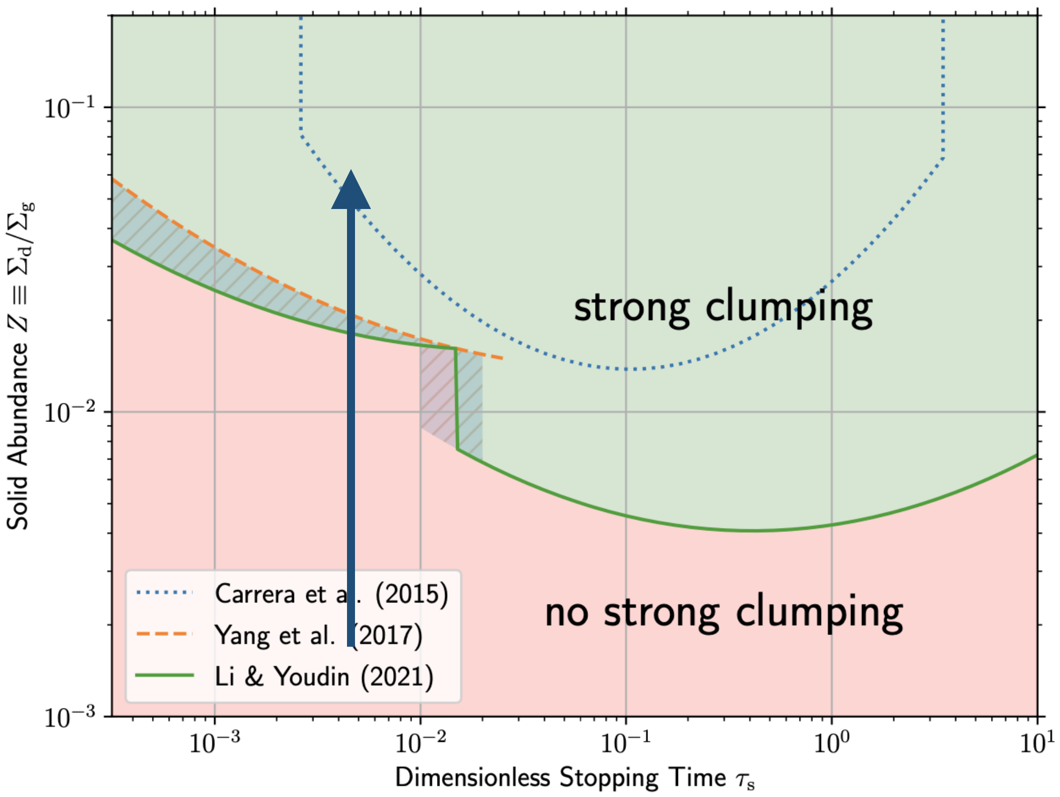

Low Metallicity + Vortex Boost

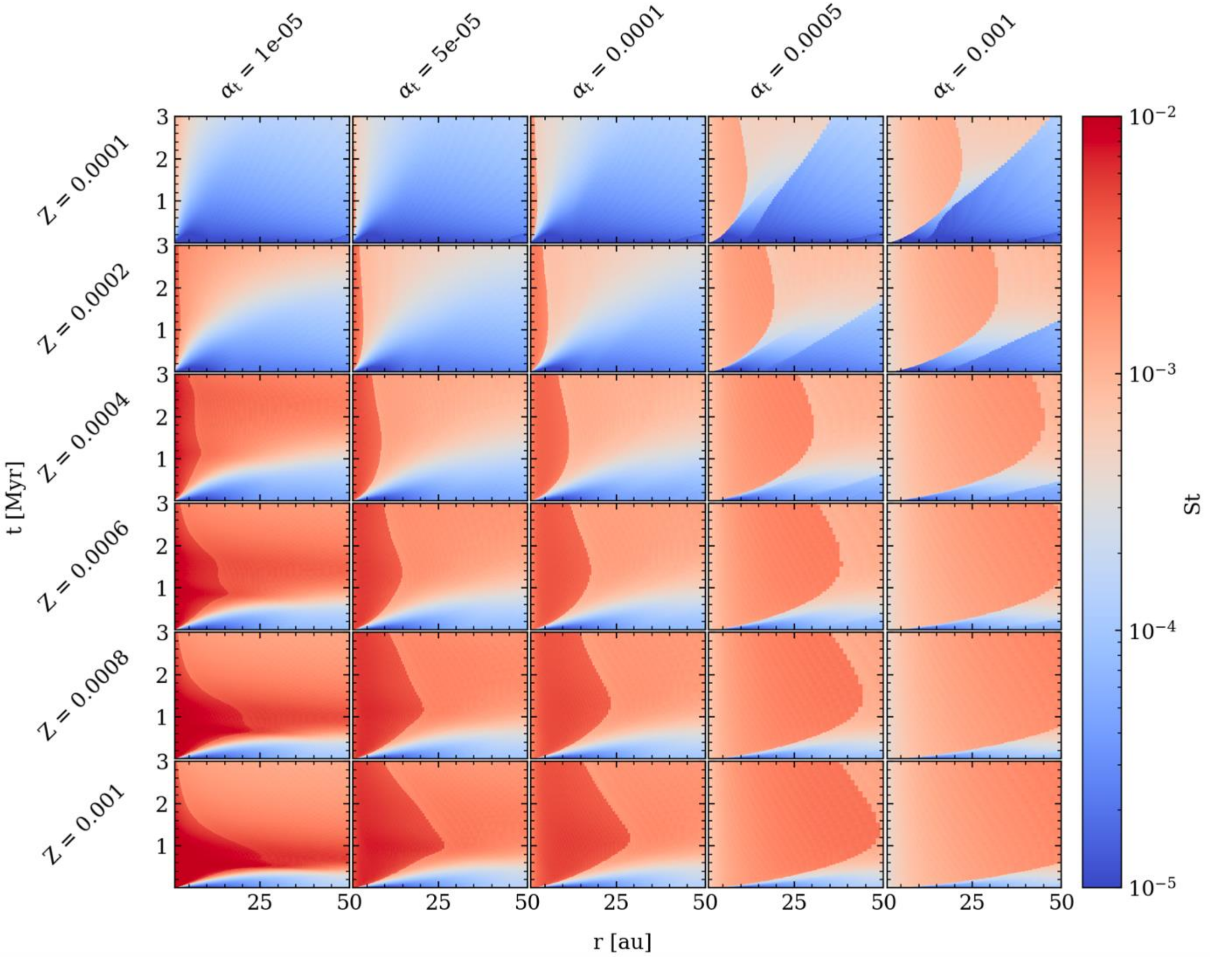

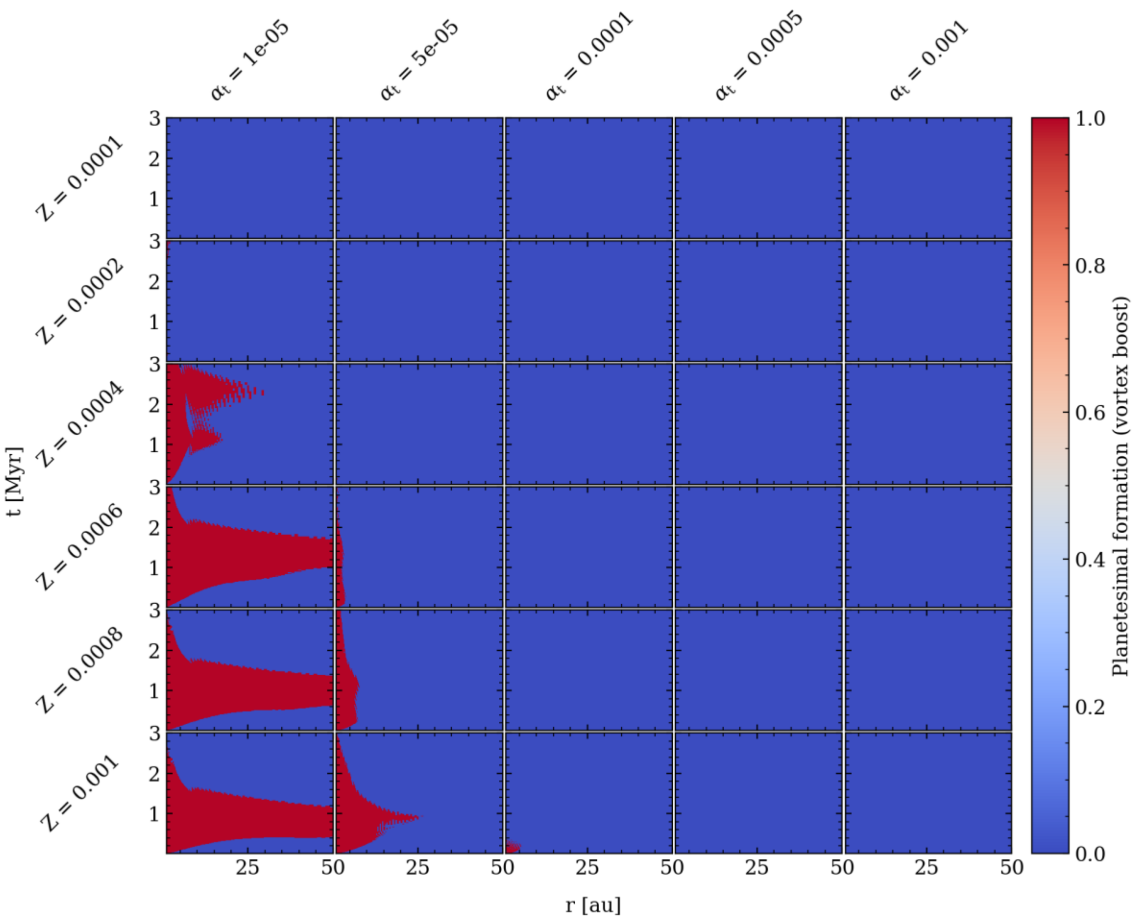

Vortex Boost – Effect on St and δ

$$Z = Z_0 \left({}^{St}/_{\delta} + 1 \right)$$

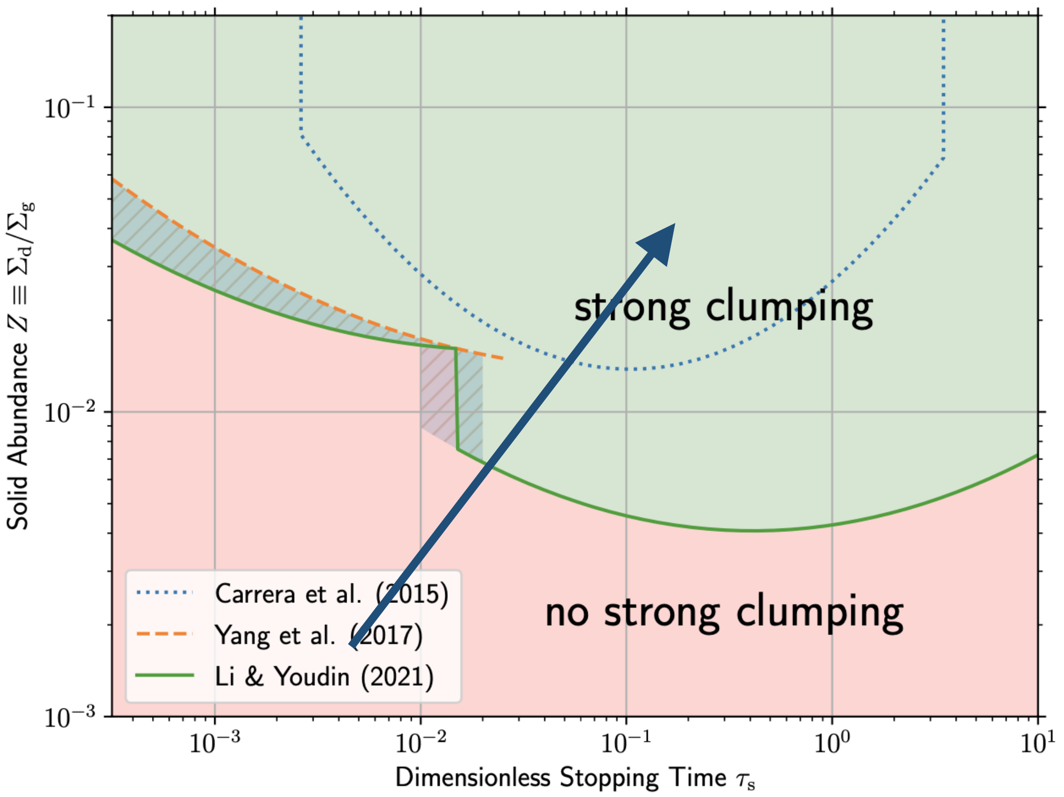

Positive feedback loop

Vortex trapping increases pebble density
Pebbles dampen turbulence
Lower turbulence increases vortex trapping

Low turbulence decreases fragmentation
Less fragmentation increases pebble size (St)
Larger pebbles concentrate further

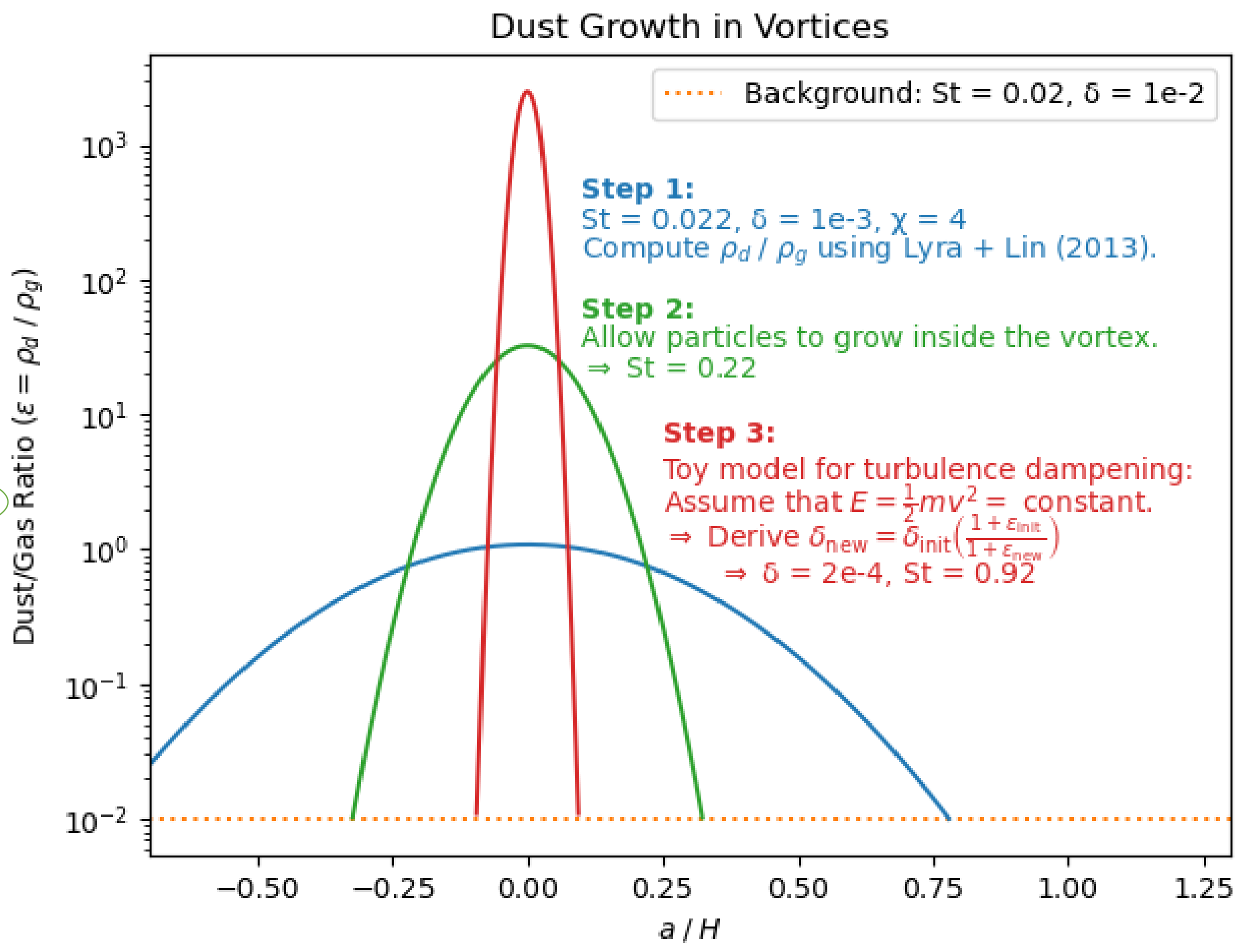

Carrera et al. (in prep)

When does the positive feedback loop stop?

Very large grains don't get trapped

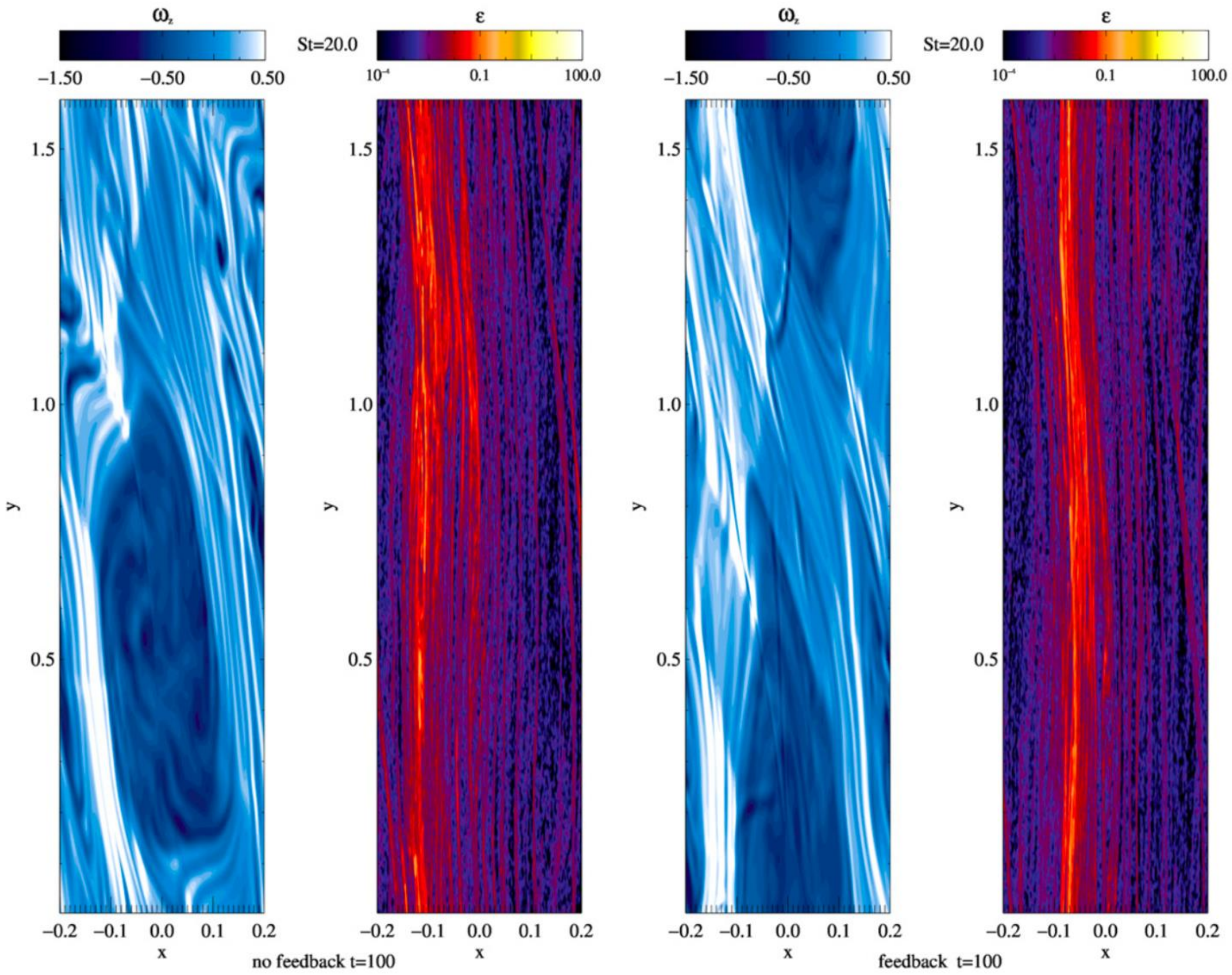

Raettig et al. (2015)

When does the positive feedback loop stop?

Fragmentation at St ~ 1

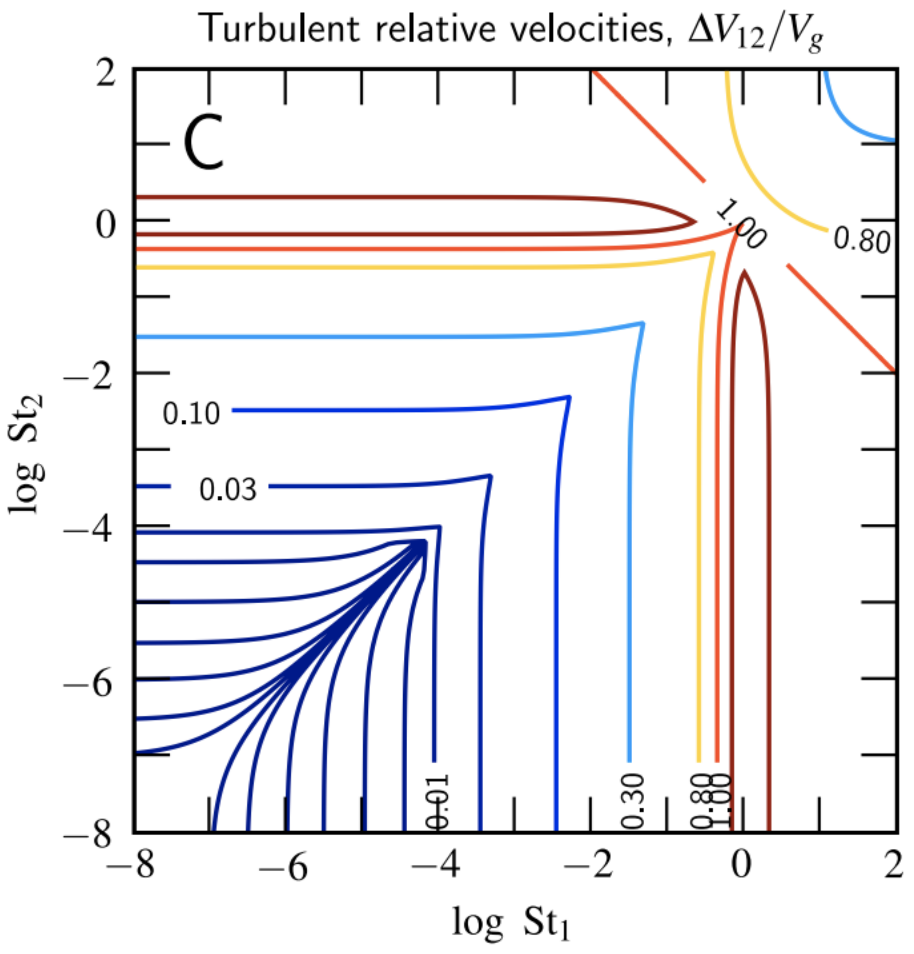

Ormel & Cuzzi (2007)

Vortex Boost – Effect on St and δ

$$\rho_{d,crit} / \rho_g = Z_{crit} ({}^{St}/_{\delta} + 1)^{1.5}$$

$$Z_{crit} \sim 6\ \delta^{1.5}$$

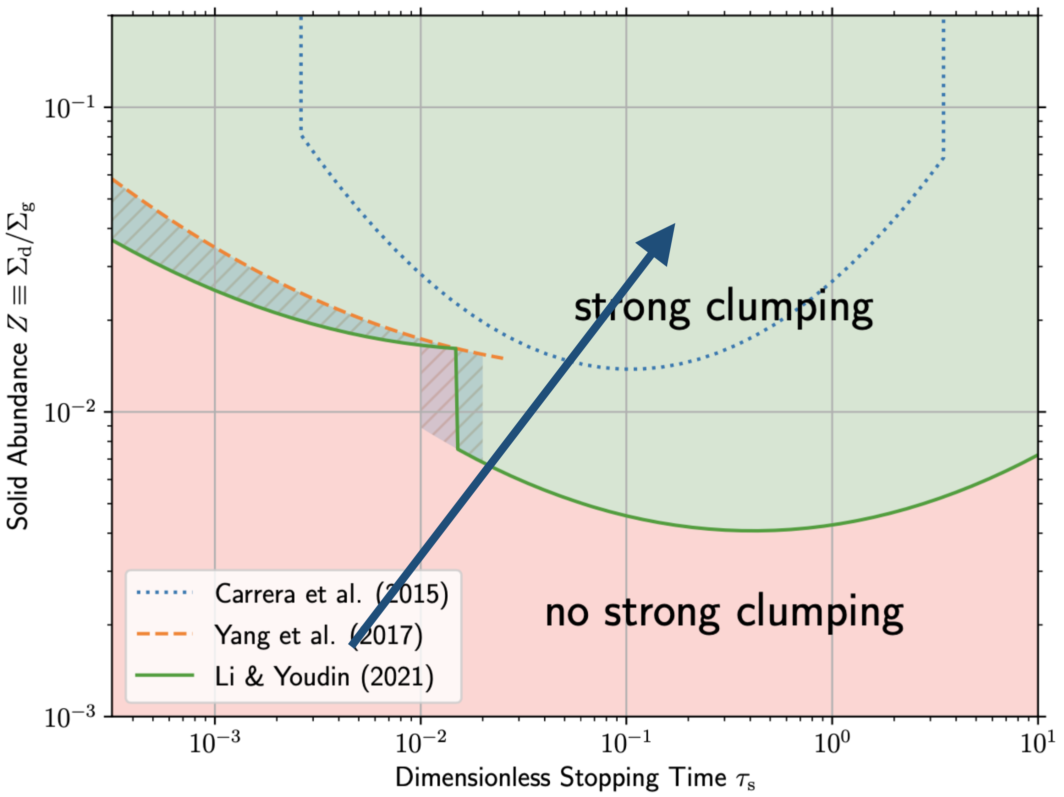

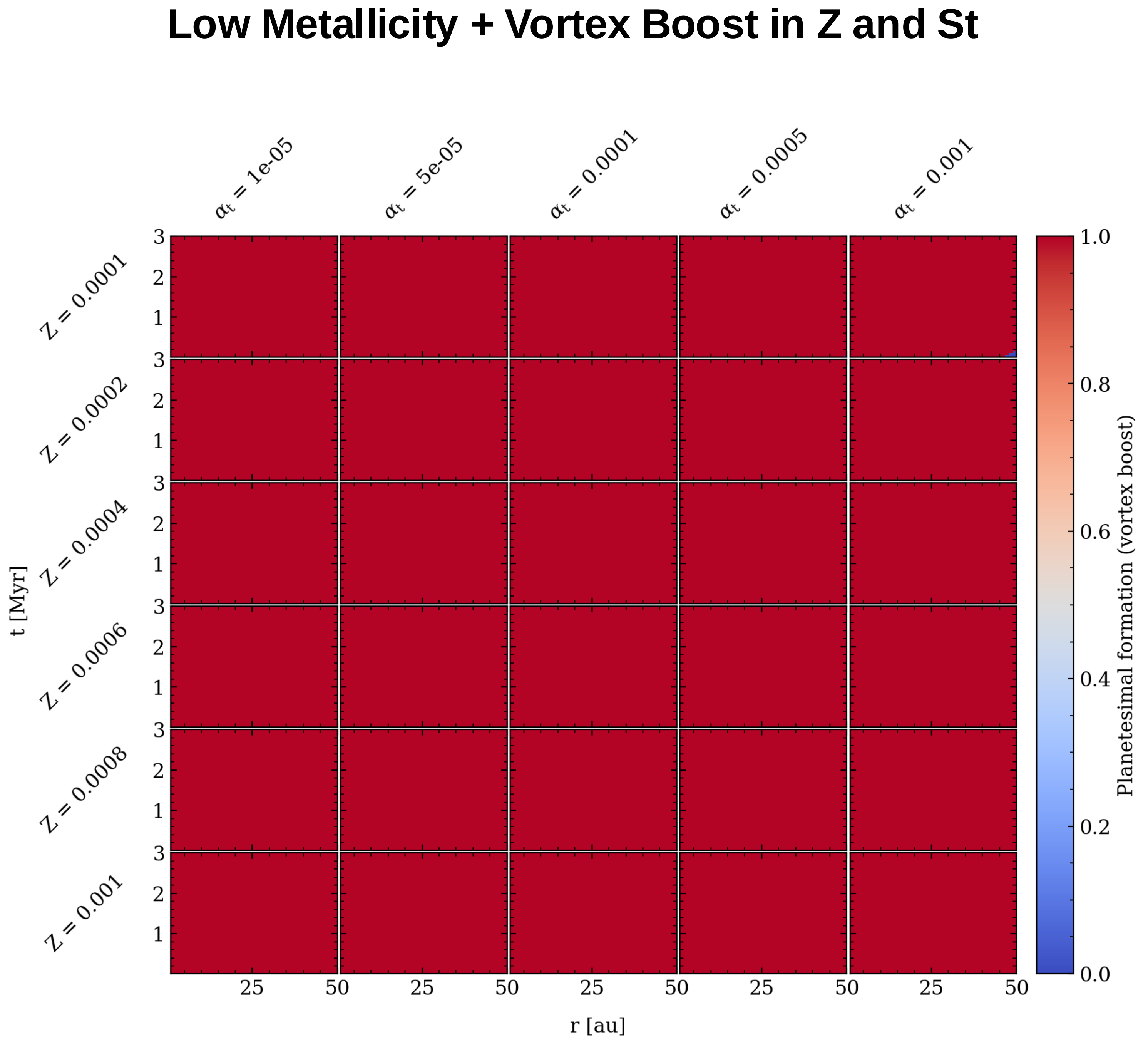

Low Metallicity + Vortex Boost in Z and St
α_t = 1e-05
α_t = 5e-05
α_t = 0.0001
α_t = 0.0005
α_t = 0.001
Z = 0.0001
Z = 0.0002
Z = 0.0004
Z = 0.0006
Z = 0.0008
Z = 0.001
t [Myr]
r [au]
Planetesimal formation (vortex boost)

$$Z_{crit} \sim 6\,\delta^{1.5}$$

$$\int \rho_d(a,z)\,dV = (2\pi)^{3/2}\ \varepsilon\ \rho_0\ \chi\, H\, H_g^2$$

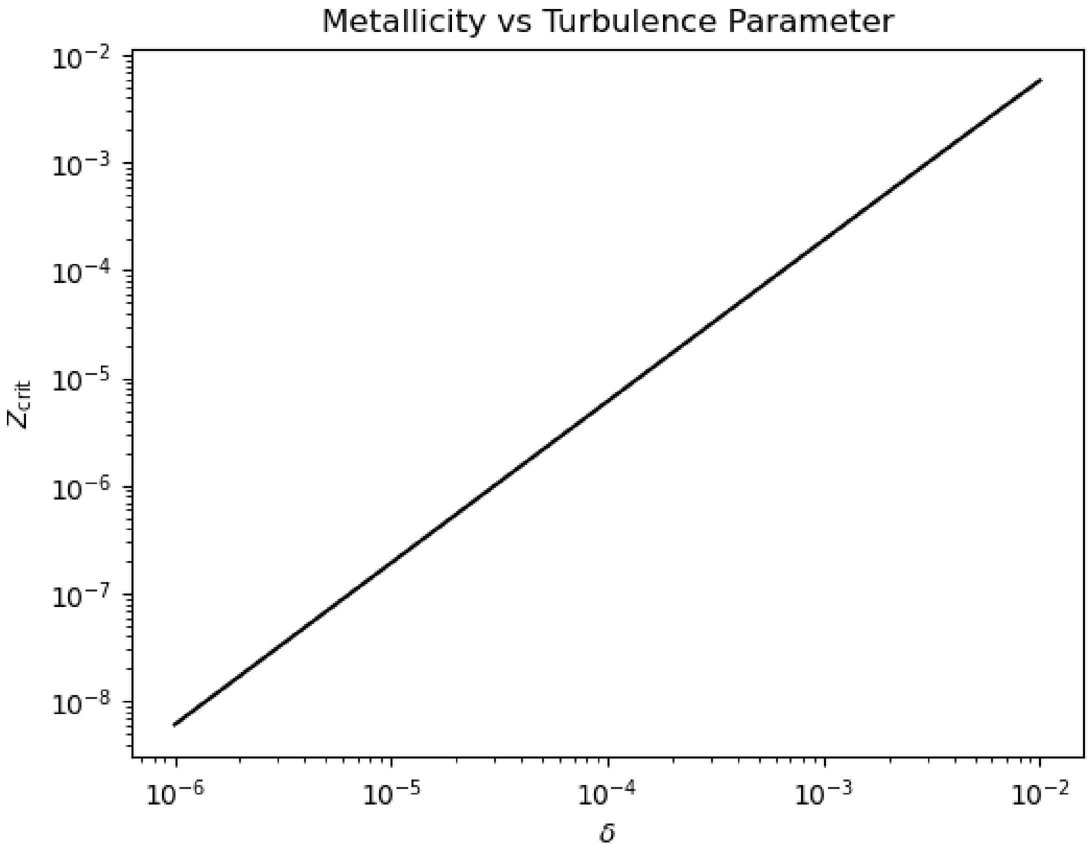

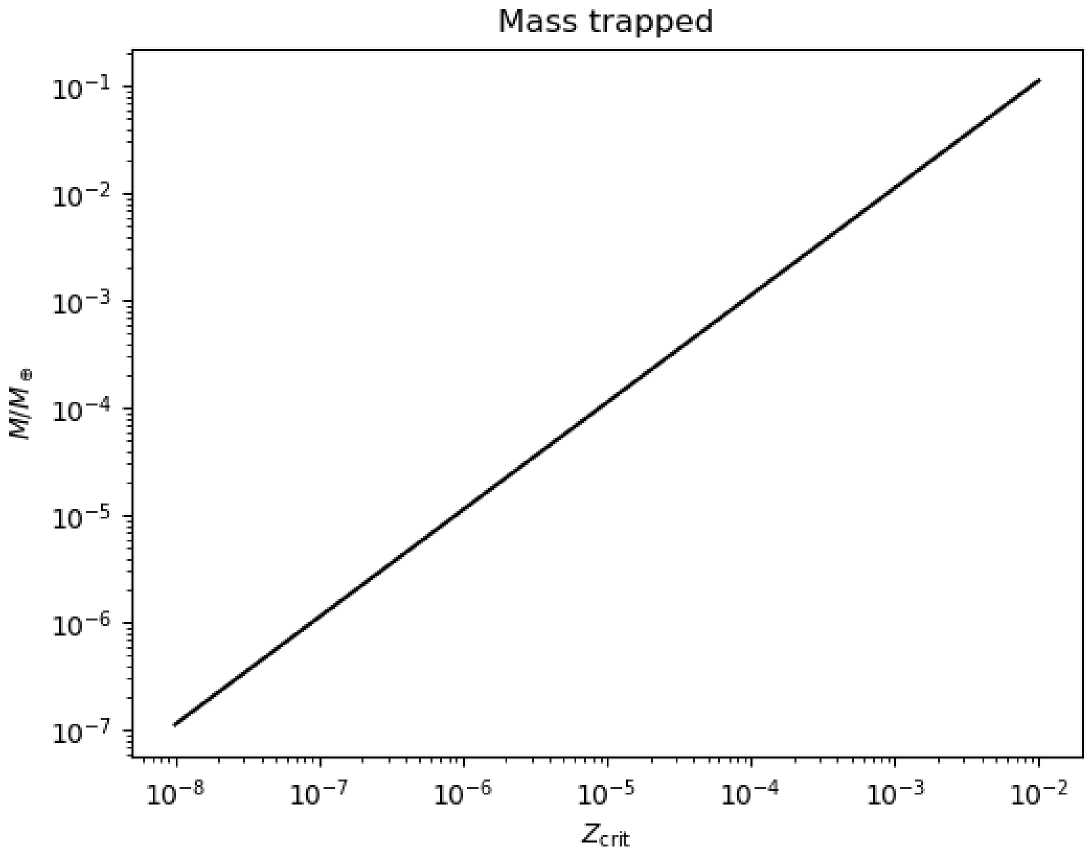

Conclusions

- **Vertical Shear Instability and Convective Overstability may be relevant for planet formation**
  - Vertical Shear Instability: rapid cooling + radial temperature gradient
  - Convective Overstability finite cooling time + radial entropy gradient
  - Saturate into vortices

- **Vortices are very efficient pebble traps**
  - High particle load disrupts vortical motion around midplane, but not the full column
    - Trapping properties are retained
  - The pebble load is high enough to lead to direct gravitational collapse

- **Planet population is of planetary embryo mass**
  - Moon to Mars mass objects
  - Resolved simulation in both gas and pebbles

- **Limitations**
  - Streaming Instability not resolved
  - Coagulation/Fragmentation not modeled